Kinetic Analysis of Cryotropic Gelation of Poly(Vinyl Alcohol)/Water Solutions by Small-Angle Neutron Scattering

Claudio De Rosa, Finizia Auriemma, and Rocco Di Girolamo

Contents

Abstract Aqueous poly(vinyl alcohol) (PVA) solutions subjected to cryogenic treatment form strong physical gels. The cryogenic treatment basically consists of freezing an initially homogeneous polymer solution at low temperatures, storing in the frozen state for a definite time, and defrosting. These gels are of great interest for biotechnology, medicine, the food industry, and many other applications. The outstanding properties of these systems depend on a complex macroporous architecture, whereby PVA chains and water molecules are organized over different hierarchical length scales. The structure and the principal processes subtending the formation of these systems are discussed in the framework of our current understanding of polymer gels. These processes involve formation of ice crystals, PVA

C. De Rosa • F. Auriemma (✉) • R. Di Girolamo
Dipartimento di Scienze Chimiche, Università di Napoli Federico II, Complesso Monte Sant' Angelo, via Cintia, 80126 Napoli, Italy
e-mail: finizia.auriemma@unina.it

O. Okay (ed.), *Polymeric Cryogels*, Advances in Polymer Science 263,
DOI 10.1007/978-3-319-05846-7_4,

crystallization, liquid–liquid phase separation, hydrogen bonding, and entanglements. Small angle neutron scattering is used to follow the cryotropic gelation of PVA/water solutions and detailed information is extracted concerning the gelation mechanism and kinetic parameters related to the formation of these complex systems.

Keywords Cryotropic gelation • Poly(vinyl alcohol) hydrogels • Time-resolving small angle neutron scattering • Ostwald stage-rule • Confined polymer crystallization

Abbreviations

a-PS	Atactic polystyrene
BP	Berghmans point
CLSM	Confocal laser scanning microscopy
C_p	Polymer concentration
$^{d\sigma}/_{d\Omega}$	Scattering cross-section
d_s	Surface fractal dimension
DSC	Differential scanning calorimetry
F	Free energy
$\langle \Phi \rangle$	Order parameter
f_c(DSC)	Fractions of crystalline phase from DSC analysis
f_c(NMR)	Fraction of rigid protons from NMR measurements
f_c(XR)	Crystallinity index from WAXS analysis
LL	Liquid–liquid phase separation
NMR	Nuclear magnetic resonance
PEG	Poly(ethylene glycol)
PVA	Poly(vinyl alcohol)
q	Scattering vector
SANS	Small angle neutron scattering
SEM	Scanning electronic microscopy
TEM	Transmission electron microscopy
T_g	Glass transition temperature
T_m	Melting temperature
TR-SANS	Time resolving-SANS
UCST	Upper critical solution temperature
WAXS	Wide angle X-ray scattering

1 Introduction

In this chapter, we deal with kinetic and mechanistic aspects associated with the complex cryotropic gelation of semidilute aqueous solutions of poly(vinyl alcohol) (PVA). The possibility of obtaining strong physical gels by cryogenic treatments of PVA/water solutions has been well known since the 1970s [1–6]. The cryogenic treatment basically consists of freezing an initially homogeneous polymer solution at low temperatures, storing in the frozen state for a definite time, and defrosting. Freezing is generally performed at high cooling rates and, in order to improve the strength of the gels, freezing and thawing are repeated a number of times. The strength of PVA cryogels prepared by means of freeze–thaw cycles depends on the initial polymer concentration in the solution to be frozen, the thawing rate, the permanence time of the solution at low temperatures, and the number of imposed freeze–thaw cycles. Cryogel strength is virtually independent of the temperature of freezing and the cooling rate of the initial solution to that temperature [4, 5, 7]. Strong physical gels can be obtained even by imposing a single freeze–thaw cycle, either with use of slow thawing rates or by the prolonged storage of the samples at subzero temperatures [3].

The large interest in PVA cryotropic hydrogels is due to a number of unique properties, including high dimensional stability, large deformability, maintenance of high conservative elastic modulus even after immersion in water for a long time [8, 9], and self-healing performance [10]. In addition, the well-tested biocompatibility of freeze–thaw PVA hydrogels and their ability to incorporate and release large amounts of host molecules of different size in their structure make these systems particularly attractive for biomedical and biotechnological applications [1, 5, 11].

The outstanding physical properties of freeze–thaw PVA hydrogels derive from their complex structure, whereby PVA chains and solvent molecules are organized at different hierarchical length scales. These gels exhibit a structure that includes an interconnected network of micro- and macropores filled by a polymer-poor phase. The network scaffolding is ensured by interconnected regions of a polymer-rich phase [1]. The latter phase is itself organized and consists of small fringed micelle-like crystalline aggregates of PVA chains and amorphous domains. The PVA chains in the amorphous domains are swollen by the solvent and act as tie chains that connect the PVA crystallites.

Section 2 is aimed at recalling the general aspects of polymer gels. These concepts turn out to be useful in Sect. 3 for understanding the mechanism of formation, the structure, and the properties of PVA hydrogels generated by physical crosslinking processes, first in general terms, then focusing on freeze–thaw PVA hydrogels in particular. The structure of freeze–thaw PVA hydrogels is discussed in detail and possible mechanisms leading to their formations are illustrated, emphasizing some aspects that have been investigated using time-resolving analysis with small angle neutron scattering (TR-SANS). TR-SANS is used to follow the structural transformations occurring during consecutive freeze–thaw cycles, with the

aim of extracting appropriate descriptors of the structural transformations occurring at the relevant length scale and the kinetic parameters. Chemical hydrogels of PVA are not included in the present context, in spite of their importance and interesting properties in several applications. Some excellent reviews on this subject may be found in the literature [1, 12, 13]. The last section is devoted to the conclusions and outlook.

It is worth noting that understanding the factors that govern the cryogelation mechanism of homogeneous polymer solutions is useful both in fundamental studies of the phenomena subtending the formation of macroporous gels in PVA and polymers in general and from an applicative standpoint. Such knowledge can enable control of the final architecture of cryogels by simply tuning the conditions of preparation, with the aim of obtaining materials with enhanced properties for tailored applications.

2 General Considerations

Polymer gels are mesoscopic systems that include a liquid phase (solvent) and a crosslinked three-dimensional (3D) polymer network intimately swollen by the solvent (solvate) [14–16]. The two phases cannot be distinguished at macroscopic level, meaning that the gels at macroscale are homogeneous systems.

Gels, are generally formed starting from a solution of a low or high molecular mass precursor (sol) as a result of a crosslinking process that is able to create a macroscopic 3D network (gel). Because the presence of crosslinks reduces the mobility of the molecular species that have reacted to become part of the network, the solvent may end up entrapped within the network-gel in high amounts instead of being rejected. It is worth noting that, although the solvent may largely exceed the polymeric component by weight, gels do not behave as viscous polymer solutions, but rather behave as elastic solids or semisolids able to withstand their own weight, even over long time scales.

The liquid component of a gel may either be a pure solvent of the initial precursor or a polymer-poor liquid phase. The mobility of the solute and solvent molecules in these liquid domains is high, as in a solution. Consequently, gels combine the properties of a solid network structure and a liquid solution at the mesoscale level, giving rise to materials with unique properties that are useful for a variety of applications.

In particular, polymer gels (depending on the chemical constitution of the components, processing conditions, and phase composition) may feature a gamut of properties that range from those of hard and tough materials to those of elastomers, that is, they are able to undergo large deformation upon application of pressure and to quickly recover the initial shape and dimensions when the external stress is removed [12–18]. In all cases, the high dimensional stability of gels is ensured by the presence of a network, which can be built by either physical or chemical crosslinks, giving rise to either physical or chemical gels.

Examples of physical crosslinks are microcrystalline aggregates, entangled chains, ionic interactions between charged atoms or groups of atoms, and hydrogen bonds. Physical gels are also reversible because the physical crosslinks can be created and removed by appropriate physical stimuli (e.g., pH, contact with a nonsolvent, etc.), and, typically, temperature. For this reason, they are often named "thermoreversible."

In chemical gels, the crosslinks are covalent bonds connecting the arms of the 3D network. As a result of covalent bonding, chemical gels are irreversible.

Whereas chemical gels are generally strong, physical gels may be strong or weak, depending on the strength of the interactions involved in the crosslinks. Strong physical gels have strong physical crosslinks between polymer chains that are effectively permanent for a given set of experimental conditions [15–17, 19]. As an example, strong physical junctions may consist of glassy or microcrystalline nodules, triple helices, or coiled-coils as, for instance, in the case of hydrogels formed from fibrous proteins or biomacromolecules.

Weak physical gels have reversible links formed from temporary weak interactions between chains, of the order of kT. These associations have finite lifetimes, breaking and reforming continuously. Examples of weak physical bonds are hydrogen bonds, ionic associations, and micellar aggregates of block copolymers.

The outstanding physical properties of gels associated with their fast stimuli response have noticeably stimulated research for a long time. Polymeric gels have been developed that are "smart," i.e., able to quickly respond to different external stimuli [15, 20]. For instance, Tanaka's gels have valuable applications because they can expand and contract up to 1,000 times their original volume in response to external stimuli. These gels could be used as artificial muscles, set in motion by a specific electric pulse [21]. More importantly, the polymers in the gels can capture or expel specific substances as they grow or shrink, so that the gels could be used, for example, as super-sponges to absorb and immobilize toxic waste, or as molecular filters of various sorts [18, 20–23]. Among the smart gels, there are materials that imitate proteins by recognizing conditions and responding to their environment. For example, smart gels can be fine-tuned to draw humidity from the air when it is over a certain level at a given temperature. Other gels can release insulin when the glucose level in the water-rich phase drops below a given point [15, 18]. Moreover, it is worth remembering that gels represent an important intermediate step in polymer processing for obtaining highly oriented fibers showing high strength and high modulus (e.g., ultrahigh-strength polyethylene fibers Dyneema and Spectra) [17].

The outstanding properties of gels are directly related to the chemical nature of their constituents, their reciprocal arrangement and interactions, and their mobility in the space. Structure and mobility in a gel, in turn, are fixed by the preparative conditions and processing. Although a gel may be assimilated to a single giant branched macromolecule, the structure of its parts covers different orders of hierarchical organization on different length scales. Roughly, the hierarchical apparatus of gels ranges from a few nanometers for the size of knots; to hundreds of nanometers for the organization of matter between first neighboring knots; to

microns for the relative organization of clusters of knots; and so on. Gels may include macro- and/or microscale heterogeneities such as macro- and micropores inside their structure. The length scales and the kind and degree of heterogeneities in a gel have a strong influence on its final properties. Therefore, the design of preparation/processing methods for achieving gels with tailored morphology able to ensure prefixed properties is a research area of great applicative interest.

From a fundamental point of view, the achievement of this goal needs the establishment of precise relationships between the functionality of the gel and its fundamental constituents, their chemical nature, their geometric arrangement, and their mobility. Of primary interest in basic research in the field of polymer gels are (1) definition of the structural organization of gel components on different length scales and (2) the structural and morphological transformations of a gel in the initial state (preparative ensemble), during its performance under application of external stimuli on the proper time scale (applicative ensemble), and in the final state (end use ensemble) [24]. In the present context we focus on gels in the preparative ensemble.

2.1 Physical Gels in the Preparative Ensemble: Main Processes Creating Networks

Physical gels may originate from a large number of processes able to create junctions (Fig. 1). Each one of these processes may act alone or in synergy with the other processes to induce the sol–gel transitions (gelations). Gelation is not a first-order phase transition and does not lead to a state of thermodynamic equilibrium [16]. Instead, the kinetics of the process and the way a crosslinking process is activated play key roles in the transition [17, 25].

As shown in Fig. 1, sol–gel transitions may be easily driven by the entanglements established among the polymer chains in a semidilute or concentrated homogeneous solution , i.e., at concentrations higher than that occupied by each polymer coil within its own pervaded volume, corresponding to the overlap concentration [19]. This means that polymer random coils should overlap in order to establish an entangled network [24] and, hence, to form a gel.

Besides entanglements, a second kind of crosslinking process leading to gelation involves physical associations such as polar–polar interactions, ionic forces, colloid interactions, hydrogen bonding, or complex associations such as formation of multiple helices and/or coiled-coils in biopolymers, self-assembly with formation of micellar aggregates in amphiphilic block copolymers, and so on.

As shown in Fig. 1, gelation may be also driven by phase transitions as for instance crystallization. Under specific conditions, formation of crystals from a homogeneous solution can give rise to junctions and then to a gel. This happens, for example, with poly(vinyl chloride) [15], isotactic polystyrene, polyethylene [15, 26–31], and many other polymers [32]. In these gels, the junctions are constituted

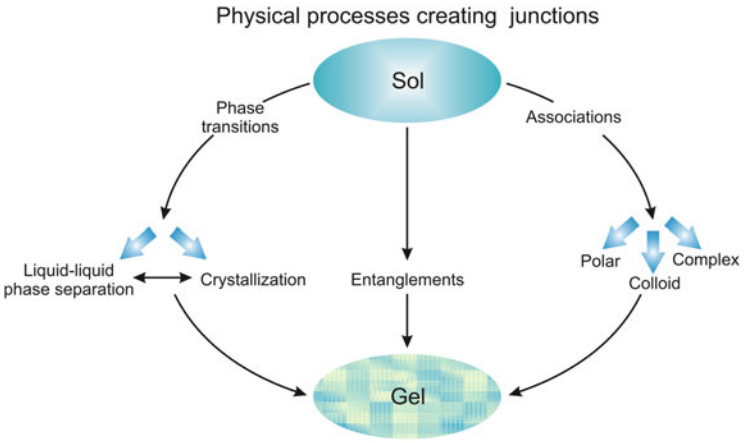

Fig. 1 Different processes able to produce a network and therefore a physical gel, and their possible correlations [17]

by small fringed micelle-like crystals or chain-folded lamellae, while the connectivity is ensured by portions of chains connecting the crystallites throughout the macroscopic samples, swollen by the solvent.

Finally, gels may be also generated through a liquid–liquid (LL) phase separation, or a combination of LL phase separation and crystallization, as we shall see in Sect. 2.2 [17, 25].

Regardless of the kind of process, gelation involves complex mechanisms and the gradual formation of junctions [16, 19]. As long as these junctions form aggregates of small dimensions, the system is still a sol (Fig. 2a). Gel is formed when the concentration of junctions reaches a threshold value, so that at least a single aggregate having infinite size is created, that is, aggregates having the same size as the macroscopic sample (Fig. 2b). Above this threshold value some sol (aggregates of finite size, indicated with an arrow in Fig. 2b) may still survive, and these aggregates end up connected to the gel only in the later stages of the process. This is in essence the (site) percolation model [16, 19].

2.2 Metastability and Sol–Gel Transitions

In order to better understand the mechanism of formation of a 3D network, and then a gel, via a gradual crosslinking (both physical and chemical) process according to the percolative scheme shown in Fig. 2, we need to emphasize that, regardless of the processes involved in the creation of junctions, these processes compete with gelation [16, 17, 25]. As a result of this competition, the process is arrested at an intermediate level instead of proceeding to completion, so that the system does not attain the ultimate thermodynamically stable state, but reaches a state far from

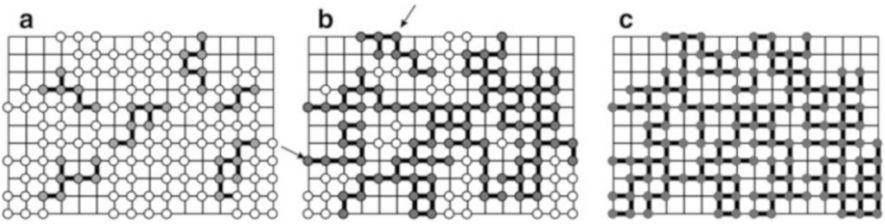

Fig. 2 Scheme of percolation in a two-dimensional network [16, 19]. Only ≈72 % of the sites are occupied by "particles" able to form a junction. Each particle may form 1–4 junctions with a first neighboring particle. *Empty balls* correspond to unbound particles, *filled balls* are the particles connected with at least one first neighbor. (**a**) Sol: The fraction of particles that have created a junction is below a threshold value. (**b**) Immediately above this threshold, we have an aggregate of infinite dimensions (i.e., the aggregate is of the same size as the macroscopic sample) swollen by the solvent, unreacted particles, and aggregates of finite dimensions (indicated by an *arrow*). (**c**) Gelation progresses to include all particles

equilibrium [17, 25]. This means that, although gels are often quite long-living with respect to the lifetime of an experiment, they are usually in a metastable state [17, 25]. For instance, in the framework of the percolation model shown in Fig. 2, for crystallization-driven gels, when the number density of crystallites that gradually form in a solution achieves a threshold value, they give rise to a percolative network extending all over the macroscopic sample, with consequent formation of a gel. Simultaneously, the crystallization process is arrested at an intermediate state far from equilibrium, namely, corresponding to a metastable state. This mechanism is valid for any process able to form junctions [17, 25].

The formation of a gel and the concept of a gel as a metastable state of matter fits quite well with the Ostwald "stage rule" [33]. This rule was formulated at the end of the nineteenth century and states that "a phase transformation from one stable state to another proceeds via metastable states, whenever such states exist, in stages of increasing stability." Although this rule does not explain why phase transitions evolve in this way, it is considered an intrinsic property of matter.

A metastable state of matter is a state that can exist on the basis of the laws of thermodynamics and is stable with respect to infinitesimal fluctuations, yet it does not represent the state of ultimate stability. In Fig. 3, the free energy, F, is reported as a function of an "order parameter" $\langle \Phi \rangle$. It is apparent that both metastable (M) and ultimate stable (E) states are such that the first derivative of F with respect to $\langle \Phi \rangle$, $dF/d\langle \Phi \rangle$, is equal to zero, and the second derivative ($d^2F/d\langle \Phi \rangle^2$) is positive. Evolution from the metastable state M to the equilibrium state E needs activation, ΔF. Although a metastable state will evolve to an equilibrium state sooner or later, its lifetime may be longer than the timescale of the experiment [17, 25].

At this point, it is important to introduce two different classes of metastability: classical metastability and circumstantial metastability [25].

A kind of classical metastability occurs in the case of thermodynamic phase transitions, as for instance in the case of an LL phase separation. Here, the order parameter $\langle \Phi \rangle$ may be identified with the polymer concentration. Fig. 3 states that at

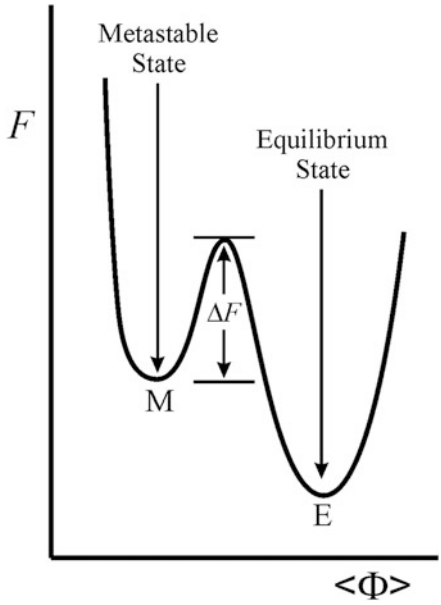

Fig. 3 Scheme of a metastable state (M) in a plot of the free energy F as a function of the order parameter $\langle \Phi \rangle$. ΔF represents an activation barrier bringing the system from the metastable state M to the equilibrium state E [33]

a given concentration (and temperature) a solution in a state of metastability M may reach the equilibrium state E corresponding to phase separation, only by crossing a barrier ΔF able to create nuclei of the two phases. The nuclei, once formed, grow, thus decreasing the free energy and the system reaches the ultimate state of thermodynamic equilibrium at its own pace.

The concept of circumstantial metastability [25] comes into play in the case of gels. Here, the order parameter $\langle \Phi \rangle$ may be identified with the gel fraction, i.e., the fraction of "particles" (i.e., molecules, bonds, chains, portion of chains, etc.) in Fig. 2 attached to a macroscopic aggregate during its development. If we assume that all particles have a functionality of 4 in the square lattice of Fig. 2, each particle is expected to form a connection with all particles located in the first neighboring sites in the final state. However, in the configuration of Fig. 2c it is evident that some particles are connected with only two or a maximum of three of the available first neighboring particles. Therefore, the system in Fig. 2c is far from equilibrium; it is in a metastable state, and can attain a state of lower free energy only by crossing a thermodynamic barrier. The reason why it may assume a frozen-in configuration such as that in Fig. 2c can be explained by kinetics. Some agency able to create metastability comes into play [25], reducing the "reactivity" of the particles and freezing the gel in that configuration. The nature of the agency able to create a metastable state in a sol–gel transition could be the presence of impurities blocking the functionality of some particles, the high viscosity achieved by the system at onset of gelation, the temperature, and many other factors.

2.3 Role of Phase Separations in Gel Formation

The arguments of Sect. 2.2 mean that two specific conditions must be fulfilled in order for a phase transformation to lead to a macroscopic network of junctions and thus to a gel [17]: first, the phase transformation must be incomplete and, second, it must stop wherever connectivity has been established throughout the whole macroscopic sample.

The first condition is driven by thermodynamics, but it is always controlled by the kinetics of the process through some kind of agency able to create metastability [25]. Because of this agency, the system fails to attain its ultimate stability (corresponding to completion of the process) and is arrested in one of the multiple minima of the free energy profile with respect to the order parameter $\langle \Phi \rangle$ (Fig. 3).

The second condition is a geometric factor and it is not related to the process, but represents the *condicio sine qua non* for obtaining a gel. It is worth noting that the connectivity can be established either by individual chain molecules or by a continuity of microphase separated domains, or by a combination of both kinds of associations [25]. As a consequence, a large variety of morphologies may be obtained, depending on the chemical nature of the polymer, the kind of solvent, the initial polymer concentration, the gelation temperature, the rate of cooling/heating to this temperature, and so on.

Although application of the above general concepts to understand physical gelation is, at least on a qualitative ground, straightforward in the case of crystallization, it is more tricky in the case of LL phase separations.

LL phase separation may play a key role in the gelation of some noncrystalline polymers such as atactic polystyrene (a-PS) [34–36]. For a-PS, the physical junctions are not crystals and there are no specific interchain interactions, yet a-PS can form gels. Arnauts and Berghmans were the first to explain the gelation of a-PS in terms of LL phase separation combined with vitrification [36]. In this case, vitrification acts as the agency responsible for arrest of the LL phase separation, and locks the system in a metastable state.

This mechanism is illustrated in Fig. 4a, where the phase behavior of a polymer solution featuring an upper critical solution temperature (UCST) behavior at T_c is shown as an example, with T_c being the critical temperature. Curve b in Fig. 4 is the binodal, i.e., the curve delineating the concentration of the polymer-rich and polymer-poor phases in equilibrium at each temperature. The LL phase separation occurs at temperatures below the binodal, in any case at temperatures below the T_c. In Fig. 4, the curve s represents the spinodal, which is the ultimate thermodynamic limit of stability for homogeneous solutions. Below this curve, homogeneous solutions are unstable and undergo phase separation due to the effect of infinitesimally small fluctuations in composition and density (spinodal decomposition). For concentrations that fall in the region between the spinodal and binodal, homogeneous solutions are in a (classical) metastable state, that is, they are stable with respect to concentration and density fluctuations, and undergo phase separation by a free-energy-activated process involving nucleation and growth. Finally, curve g in

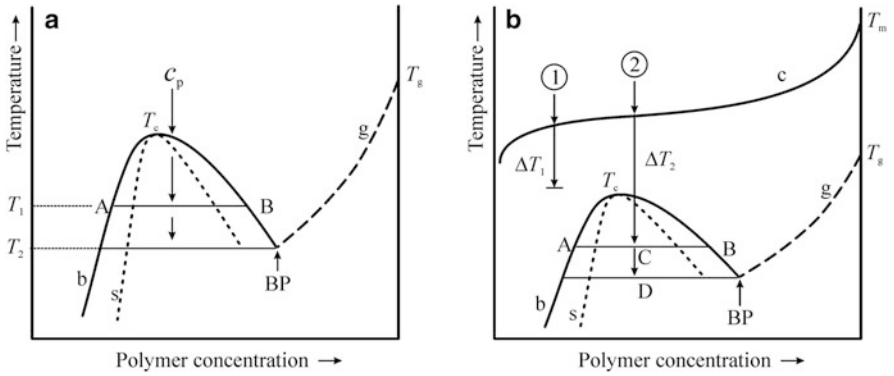

Fig. 4 Schematic phase diagrams of a polymer solution showing LL phase separation with UCST behavior. *Curve s* is the spinodal, *curve b* is the binodal, and *curve g* is the glass transition temperature as a function of polymer concentration. *BP* indicates the Berghmans point. (**a**) LL phase separation is the only thermodynamic transformation of the system [17, 25, 36]. (**b**) *Curve c* shows the crystallization temperature of a polymer fully miscible in a solvent as a function of concentration in the solution [17, 25]. The LL phase coexistence curve (combined with vitrification) is a (classical) metastable process that lies beneath the crystallization curve *c*. In route *1*, a polymer solution is supercooled at ΔT_1, and the only active process is polymer crystallization. In route *2*, the initially homogeneous solution is supercooled to a larger undercooling than ΔT_1, namely ΔT_2. Crystallization may compete either with LL phase separation when reaching point *C*, or LL phase separation coupled with vitrification when reaching point *D*. At *C*, crystallization may take place in the polymer-rich phase. At *D*, both LL phase separation and crystallization may become arrested by vitrification

Fig. 4 represents the dependence of the glass transition temperature T_g, on the polymer concentration. Because T_g of the pure polymer decreases by addition of the solvent, curve g intersects the binodal at the point BP, named Berghmans point after Hugo Berghmans [36].

Starting from a homogeneous polymer solution with concentration C_p, the LL phase separation sets in by decreasing the temperature below T_c, for instance, at temperature T_1. The tie line (isotherm) intersects the binodal at points A and B (see Fig. 4), and these points define the concentrations of the polymer-poor and polymer-rich phases in equilibrium at T_1, originating from the LL phase separation.

We recall that, regardless of the exact mechanism leading to phase separation (spinodal decomposition or nucleation and growth), the ultimate stable morphology obtained upon de-mixing should correspond to a two-layered liquid in order to minimize the specific interfacial area [37]. Spinodal decomposition is driven by spontaneous barrier-free composition fluctuations, so that, since the beginning and during the transient stages of the transformation, the morphology is characterized by a kind of a bi-continuous network of the two phases. By contrast, in the case of nucleation and growth, droplets of one phase are formed in the continuous matrix of the other phases before reaching macroscopic segregation. Therefore, during the de-mixing process a gamut of morphologies develops, gradually leading to the coalescence of the small domains of the two phases into increasingly bigger

domains, up to the ultimate layered morphology. The transient morphologies depend not only on the initial concentration and temperature, which in turn define the relative amount of the two phases in equilibrium based on the lever rule [19], but also on the degree of evolution of the phase separation and, hence, on the time of observation [25].

At temperatures lower than T_1, the intersection point B shifts towards higher concentrations up to reach the Berghmans point BP at T_2 (see Fig. 4). At this point, the polymer-rich phase vitrifies, blocking the progress of the phase separation. A first direct consequence of vitrification is that at and below the temperature corresponding to BP, the system ends up in a metastable state characterized by the same phase morphology prevailing at the stage of vitrification, instead of attaining the ultimate thermodynamically stable state characterized by the segregation of the two phases in layers [17, 25].

A second consequence of vitrification is that morphological development is arrested and all further compositional changes cease, and the glass transition becomes invariant with composition. If, at the moment of the arrest of LL phase separation, the vitrified phase has become connected throughout the macroscopic sample volume, the solution converts into a gel [17, 25]. Possible limiting morphologies of these gels are illustrated as an example in Fig. 5.

Gels may also arise from a combination of LL phase separation coupled with crystallization [17, 25]. This is a more complex situation and occurs when one or more metastable states lie "buried" beneath the state of ultimate stability in the phase diagram [17, 25]. A hierarchy of metastability arises in this case due to the possibility of several metastable phases. These metastable phases, once formed, can evolve faster than the transition leading to the ultimate stable phase and can dominate the whole transformation process.

As an example, Fig. 4b illustrates the case of a fully miscible polymer solution, in which polymer crystallization takes place at equilibrium values of temperatures delineated by the curve c. Hence, for this system, at temperatures below the curve c, the crystalline state corresponds to the state of ultimate stability. However, the system in Fig. 4b also displays a metastable LL phase separation, as indicated by curve b, lying below the crystallization curve c. Also shown is the glass transition temperature T_g of the polymer as a function of polymer concentration intersecting the binodal at the Berghmans point BP. A first set of metastable states may arise because of the high undercooling ΔT that is generally required for crystallization to take place at practical rates. Besides crystallization, other sets of metastable states may also arise for this system, depending on the undercooling, according to a hierarchy. Such scheme fits quite well what occurs in the case of poly(phenylene ether) in cyclohexanol, as an example [38]. In Fig. 4b, route 1 shows that, starting from an initially homogeneous solution, crystallization takes place at low undercooling ΔT_1 if sufficient time is allowed. At low undercooling, only crystallization takes place. In route 2, the undercooling ΔT_2 is larger than ΔT_1 and crosses the binodal. Depending on the magnitude of the undercooling, either de-mixing occurs first and crystals are formed in the polymer-rich phase (point C) or the polymer-rich phase vitrifies at and below the Berghmans point (point D), and both

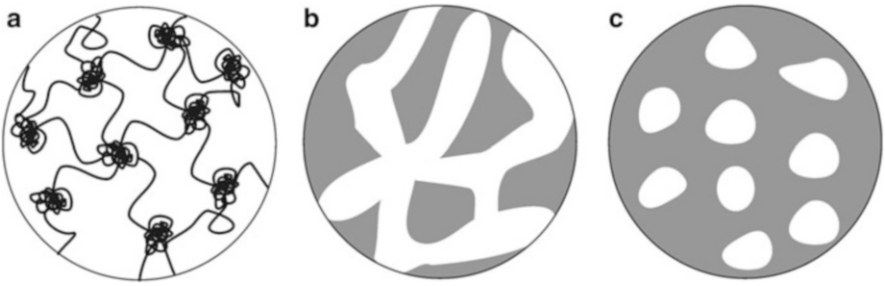

Fig. 5 Three typical frozen-in morphologies of gels obtainable by LL phase separation interrupted by vitrification: (**a**) Molecularly connected morphology comprising glassy spheres of the polymer-rich phase connected by isolated solvated chains. (**b**) Bi-continuous two-phase morphology. (**c**) Continuous glassy phase including droplets of the polymer-poor phase. The polymer-rich phase is *gray*, the solvent-rich phase is *white*. In **b**, the connectivity of the two phases could only be represented in two dimensions. For crystallizable polymers, the physical crosslinks in **a–c** may also be small crystallites, either in the shape of chain-folded lamellae or fringed micelle-like aggregates

de-mixing and crystallization processes are arrested by vitrification. In both cases, gels may be formed only if the degree of connectivity in the polymer-rich phase achieves a threshold value. Furthermore, regardless of undercooling depth, the above hierarchy of metastability may become accessible only if the initial homogeneous solution is cooled to the target temperature at high rates. For low cooling rates, crystallization is likely to occur during the cooling process before the attainment of binodal and/or vitrification. In route 1 of Fig. 4b, homogeneous gelation may take place if small crystallites are formed that are well interconnected all over the macroscopic sample by well solvated tie chains (as shown in Fig. 5a), the difference being that the amorphous nodules are replaced by chain-folded lamellae or fringed micelle-like crystals. By contrast, the structures of gels that are likely to result from route 2 of Fig. 4b are porous and heterogeneous (as shown in Fig. 5b, c). They consist of two bi-continuous phases meandering around each other, namely a polymer-rich and a polymer-poor phase. In these gels, the regions of the polymer-poor phase act as pores and allow small and large molecules to diffuse, whereas the polymer-rich regions are heterogeneous and include an amorphous phase swollen by the solvent and small crystals or glassy nodules of the polymer. The chains in the amorphous phase connect the crystallites and/or the glassy nodules constituting the physical crosslinks of the 3D macroscopic network of the gels.

3 Poly(Vinyl Alcohol) Hydrogels

PVA is one of the most studied gel-forming polymers and is able to give rise to a large variety of gels of widespread interest, using several kinds of solvents and under a large variety of preparation/processing conditions [1]. Confining our attention to PVA hydrogels, it has been shown that aqueous solutions of PVA can form gels under several conditions and that the properties of the resultant systems are largely dependent on the structure fixed by the preparative route.

In this section, after a brief discussion of the principal categories of PVA physical hydrogels in general, the PVA hydrogels obtained by cryogenic treatments are treated in detail.

3.1 Crystal Structure of PVA

PVA is an atactic polymer obtained by free radical polymerization of vinyl acetate and successive hydrolysis. The hydrolysis of poly(vinyl acetate) (PVAc) does not convert all the acetate groups into hydroxyl groups, but gives rise to PVA polymers with a partial degree of hydrolysis that depends on the extent of the reaction.

The properties of PVA are strongly influenced by the degree of hydrolysis [39]. For instance, the water solubility of PVA depends on the degree of hydrolysis and the molecular weight [12]. The higher the degree of hydrolysis of PVA grades, the lower the corresponding PVA solubility. Residual acetate groups in partially hydrolyzed PVA improve water solubility by disrupting polymer–polymer inter- and intrachain hydrogen bonding between hydroxyl groups and, consequently, promote polymer–solvent interactions [12]. In highly hydrolyzed PVA grades, the water solubility decreases due to unhindered formation of polymer–polymer interchain and intrachain hydrogen bonds between the pendant hydroxyl groups, so that establishment of effective interactions of PVA chains with the solvent are prevented.

In spite of the lack of stereoregularity, atactic PVA is a semicrystalline polymer [40, 41]. The crystal structure of PVA was resolved in 1948 by Bunn [41]. It is characterized by chains in a *trans*-planar conformation, packed in a monoclinic unit cell with $a = 7.81$ Å, $b = 2.52$ Å (chain axis), $c = 5.51$ Å, and $\beta = 91.7°$ (see Fig. 6).

The arrangement of chains inside the crystals can be described as consisting of double layers of chains running parallel to the *bc*-plane, and stacked along the *a*-axis. These double layers are defined by the hydrogen bonds established between the hydroxyl groups belonging to first adjacent chains facing along *a*. Consecutive double layers establish only weak van der Waals interactions. The degree of stereoregularity of PVA significantly affects the crystallizability, and atactic PVA is more easily crystallized than the isotactic and syndiotactic counterparts [1, 12].

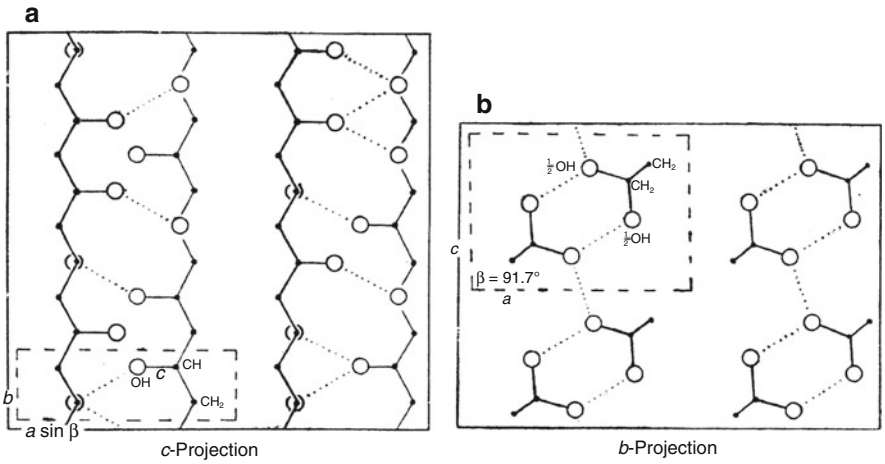

Fig. 6 (**a**, **b**) Model of the crystal structure of atactic PVA, proposed by Bunn [41] in the *c*-axis (**a**) and *b*-axis (**b**) projections. *Dotted lines* represent hydrogen bonds established between the hydroxyl groups belonging to adjacent chains along the *a*-axis within a double layer. The unit cell is indicated by *dashed lines*. Since PVA is atactic, the occupation factors of –OH groups is ½

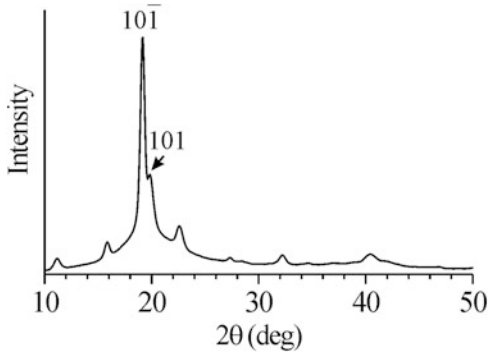

Fig. 7 X-ray powder diffraction profile of crystalline PVA. The $10\bar{1}$ and 101 reflections at $2\theta = 19.4°$ and 20°, respectively, are indicated [42]. (Reproduced with permission from [42]. Copyright 2004 by American Chemical Society)

The melting temperature of PVA ranges between 220 and 240 °C. The glass transition temperature is 85 °C in dried PVA samples [1], and decreases with the amount of water adsorbed by PVA due to plasticization effects. For instance, the glass transition temperature of PVA containing 10 wt% of water is ≈37 °C.

The wide angle X-ray (WAXS) powder diffraction profile of crystalline PVA is reported in Fig. 7 [42]. A strong peak at $d = 4.68$ Å ($2\theta = 19.4°$) and a shoulder at $d = 4.43$ Å ($2\theta = 20°$) are present, corresponding to the $10\bar{1}$ and 101 reflections, respectively, of the monoclinic unit cell [41].

3.2 PVA Physical Hydrogels

The formation of physical gels from water solutions of PVA has been widely studied. In fact, it is well known that aqueous PVA solutions undergo gelation upon cooling. In these gels, the physical cross-links are generally fringed micelle-like PVA crystallites. In particular, Komatsu et al. [43] found that the phase diagram of this system shows an upper critical solution temperature (UCST), and that the spinodal curve crosses the sol–gel transition curve. This phase diagram is redrawn in Fig. 8.

It is apparent that gelation takes place both below and above the spinodal curve, indicating that gels may be formed either accompanied by spinodal decomposition or without liquid–liquid phase separation, respectively [43]. In both cases, crystalline gels are formed where small crystals of PVA in the monoclinic form [40, 41] act as junctions [43, 44]. Statistical gels having a homogeneous structure are formed in the temperature–concentration region above the spinodal; however, the supramolecular structure of the hydrogels that develop in the temperature–concentration region below the spinodal is considerably different and more heterogeneous than the structure of the statistical gels [17, 24, 25, 43]. As discussed in Sect. 2, the development of an interconnected structure in the polymer-rich phase formed by spinodal decomposition is not necessarily the origin of gelation [17, 25]. In fact, in order to have a gel some agency should come into play to arrest PVA crystallization and/or LL phase separation at an intermediate stage, creating circumstantial metastability [25]. In the case of PVA, the network structure may be easily created by occurrence of LL phase separation, which arrests crystallization, and/or vitrification that arrests both crystallization and LL phase separation (Fig. 5b). Since the glass transition of dry PVA is equal to ≈85 °C and is lowered to ≈37 °C by the presence of ≈10 wt% water, LL phase separation of aqueous solutions of PVA are likely to occur below the Berghmans point [17, 25]. This means that PVA hydrogels formed below the spinodal may correspond to metastable frozen-in configurations affected by vitrification. Whatever the exact mechanism of gelation of PVA, the physical junctions of the macroscopic network are not only PVA crystallites, but also entanglements and hydrogen bonds.

Formation of physical gels from aqueous PVA solutions may also occur by impairing the thermodynamic quality of the solvent as a result of the introduction of nonsolvent additives [4, 5, 45]. However, in all cases, the so-obtained thermoreversible PVA gels possess low melting temperatures (T_m < 30–40 °C), low mechanical strength, and they are not able to retain their size and dimensions for a long time.

Attempts to make stronger physical hydrogels of PVA include induction of crystallization through dehydration at a slow drying rate [1, 46] and/or fast drying rate procedures such as annealing, under different conditions [1, 47]. The presence of crystals in physical hydrogels of PVA generally results in better mechanical properties than in PVA gels prepared through chemical or radiation-induced techniques.

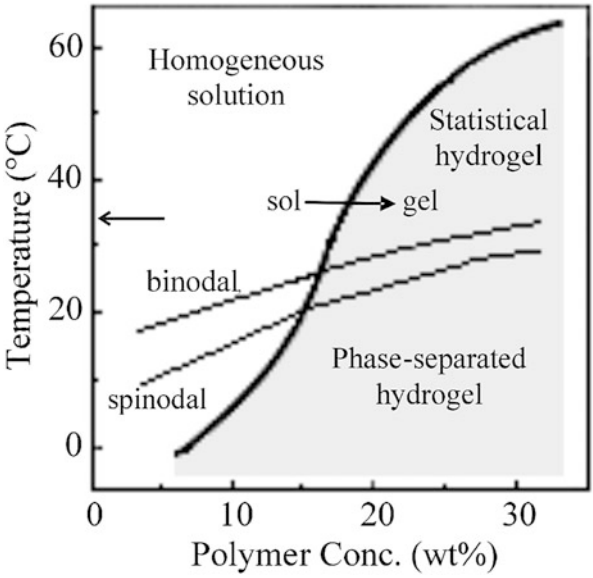

Fig. 8 Sol–gel transition curve, spinodal, and binodal of water/PVA binary system (redrawn from [43]). The *left arrow* indicates the glass transition temperature of 37 °C relative to a PVA sample that had not been dried before DSC measurement and contained ≈10 wt% water. (Reproduced with permission from [43]. Copyright 1986 by Wiley)

3.3 PVA Cryogels

In water/PVA systems, gelation may also be induced by cryogenic treatments, i.e., at temperatures where the formation of ice crystals takes place [1–7]. Cryogelation was introduced at the beginning of the 1970s as a new technique for the preparation of PVA physical hydrogels having improved mechanical properties [2, 48] with respect to those obtained using more conventional methods. As already stated in the "Introduction," this cryogenic process consists in submitting a PVA aqueous solution to repeated cycles of freezing at subzero temperature ($T < -4$ °C) and thawing to room temperature. In PVA hydrogels prepared by the freeze–thaw technique and having a rather high PVA content, the junctions in the stable supramolecular network are crystallites [1, 49].

Peppas made the first attempts to understand the freeze–thaw process of PVA solutions to form hydrogels by performing turbidimetric measurements [1, 2]. Peppas studied the gelation mechanism on water solutions with PVA content in the range 2.5–15 wt%, frozen at −20 °C for 45–150 min, and then thawed at 23 °C for long periods of time (up to 12 h). He explained the appearance of turbidity after freezing in terms of a partial crystallization of chain segments into microcrystalline aggregates. Moreover, Peppas demonstrated that crystallinity increases with increasing freezing time as well as with increasing PVA concentration [2].

Yokoyama and coworkers [49] performed X-ray diffraction experiments on PVA hydrogels. The X-ray diffraction patterns of these gels showed the presence of crystalline reflections. However, a deeper analysis of diffraction data was not

carried out because of the very low crystallinity in these systems and the presence of a broadly diffuse scattering due to the water [1, 49].

Watase and Nishinari [8] examined PVA hydrogels obtained by freeze–thaw cycles (−20 °C for 11 h, followed by 15 °C for 7 h), starting from an aqueous 15 wt% PVA solution. PVA specimens used were of five different degrees of hydrolysis, ranging from 96.0 up to 99.9 mol% hydrolyzed acetate groups. In this study, the PVA gel samples were immersed in water for 4 days before the analysis. The authors [8] reported X-ray diffraction patterns for PVA gels in the stretched and unstretched states. The X-ray diffraction profiles exhibited a halo characteristic of amorphous materials at $2\theta = 26–27^\circ$ and a weak crystalline peak at about $2\theta = 19.5^\circ$, corresponding to a d spacing of 4.53 Å. This characteristic crystalline peak was not observed for gels with a rather low degree of hydrolysis of PVA (96.0 mol%) stretched at low deformation, but it appeared at draw ratios higher than five times the initial length. The differential scanning calorimetry (DSC) thermograms of the PVA hydrogels showed an endothermic peak at about 60 °C, attributed to the disentanglements of flexible molecular chains. Another endothermic peak at higher temperature was found for all samples except for the sample prepared with PVA at the lowest degree of hydrolysis. This second peak was considered to be due to the melting of crystalline regions. The authors concluded that repeated freeze–thaw cycles as well as stretching increase the degree of crystallinity and that the elasticity is strongly affected by the latter parameter [8]. In a following study on PVA hydrogels obtained by freeze–thaw cycles, the same authors [50] pointed out by rheology, DSC, and X-ray analysis how slight differences in the degree of hydrolysis may significantly change the gel structure. They showed that the presence of bulky acetate groups can inhibit the formation of PVA gels [50].

The structure and dynamics of PVA hydrogels obtained by freeze–thaw cycles have been studied by ^{13}C NMR and ^{1}H pulse NMR methods [51–54]. Kobayashi et al. [51, 52] used high-resolution solid-state ^{13}C NMR experiments to show the role of intermolecular hydrogen bonds in the formation of PVA hydrogels through the formation of interchains crosslinks. The hydrogen bonds can be studied by observing the methine carbon lines in the immobile regions of gels; the lines can be assigned to carbons involved in two, one, and no hydrogen bonds [55]. The hydrogen bonds in the crosslinked region in PVA gels have the same NMR characteristics as those observed in the solid neat PVA. From such evidence, it was concluded that microcrystallites are formed in PVA gels.

As an example, the X-ray powder diffraction profiles of freeze–thaw PVA hydrogel samples are reported in Fig. 9 after subtraction of a straight baseline, approximating the background contribution. These gels were obtained by subjecting a 11 wt% aqueous solution of PVA to a different number of consecutive cycles consisting of a freezing step (20 h at −22 °C) followed by a thawing step (4 h at 25 °C) [42]. The as-formed PVA hydrogels obtained by one to nine freeze–thaw cycles are denoted as GEL-1 to GEL-9 samples. For comparison, the diffraction profile of pure water is also shown in Fig. 9.

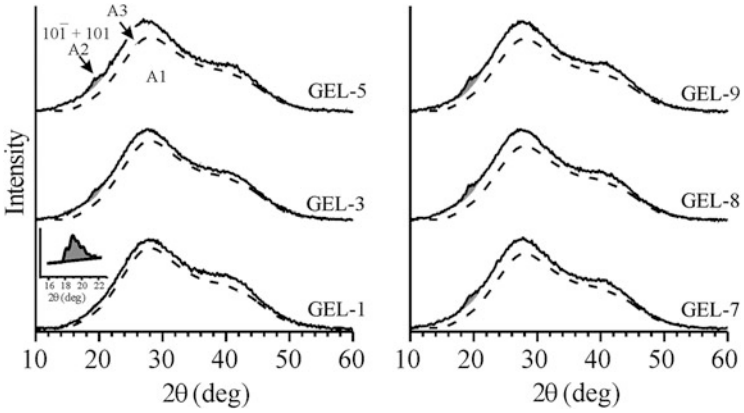

Fig. 9 X-ray powder diffraction profiles of freshly prepared PVA cryogels (samples GEL-*n*) obtained by different numbers *n* of freeze–thaw cycles (*solid lines*). The X-ray diffraction profile of liquid water is also shown (*dashed lines*). The 10$\bar{1}$ and 101 reflections of PVA crystals in the monoclinic form, in the 2θ range 18–21°, are shown in *gray*. In the case of GEL-1, the crystalline reflections are evidenced in the *inset* at an enlarged scale. (Reproduced with permission from [42]. Copyright 2004 by the American Chemical Society)

The diffraction profiles of these gels may be considered as arising from the sum of three contributions: a large contribution (region A1) derived from the pure water or a polymer-poor phase (dashed line), a small diffraction component in the range 18–21° derived from crystalline aggregates of PVA (region A2), and a third contribution (region A3) derived from the amorphous PVA phase swollen by the solvent (see Fig. 9). Therefore, at least three phases coexist in these gels: a polymer-poor phase consisting of almost pure solvent, PVA crystallites, and swollen amorphous PVA. It is apparent that the largest contribution to the X-ray diffraction scattering is due to water, whose relative amount is ≈88 % in the case of GEL-1 and gradually decreases with increasing number of freeze–thaw cycles, reaching the value of ≈85 % in the case of GEL-9 [42]. However, in all cases, the presence of 10$\bar{1}$ and 101 Bragg reflections of PVA crystals in the monoclinic form, in the 2θ range 18–21°, is the hallmark that PVA cryogels are crystalline.

The presence of crystals in PVA cryogels has been confirmed by numerous techniques, including ^{1}H NMR free induction decay experiments, and DSC analysis [56, 57].

In Fig. 10, the fractions of crystalline PVA with respect to the total amount of PVA in the crystalline and swollen amorphous phases, obtained by X-ray powder diffraction analysis, f_c(XR) [57], are reported as a function of the number of freeze–thaw cycles for the as-formed PVA hydrogels. They are compared with the fractions of crystalline PVA with respect to the total amount of PVA in hydrogels, as determined by DSC, f_c(DSC) [42, 57], and the fractions of rigid protons calculated from ^{1}H free induction decay experiments, f_c(NMR) [56, 57]. In all cases, the

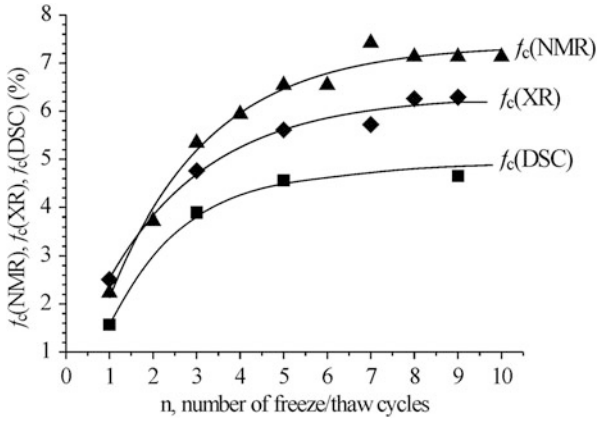

Fig. 10 Fraction (%) of crystalline PVA with respect to the total amount of PVA in the crystalline and swollen amorphous phases, obtained by X-ray powder diffraction analysis, *fc(XR) (diamonds)* [42]; fraction of crystalline PVA with respect to the total amount of PVA in hydrogels, determined by DSC, *fc*(DSC) (*squares*) [57]; and fraction of rigid protons, calculated from ^{1}H free induction decay experiments, *fc*(NMR) (*triangles*) [56, 57], as a function of the number of freeze–thaw cycles (*n*) for the as-formed PVA hydrogels. (Reproduced with permission from [57]. Copyright 2004 by the American Chemical Society)

cryogels were obtained using the same protocol, starting from a D_2O solution of 11 wt% PVA. It is apparent that the percentage of rigid PVA protons f_c(NMR) and the values of f_c(XR) are in good agreement. They both increase with increasing number of freeze–thaw cycles, from a value of 2.5 % up to a nearly plateau value after about five cycles. In particular, for GEL-9 the degree of crystallinity is around 6–7 %. The values of f_c(DSC) show the same plateau behavior after five freeze–thaw cycles, even though they are systematically lower than the values of f_c(XR) and f_c(NMR). This is due to the fact that, as a result of the small size of crystallites in PVA hydrogels and the presence of large amounts of water, in the DSC heating curves of these gels there is a strong overlap between the endothermic transition due to the melting of PVA crystals and exothermic phenomena due to PVA solubilization and solvation (or even recrystallization) [57].

More sophisticated NMR techniques have been also applied to measure the crystallinity in PVA cryogels [58]. For instance, pulsed mixed magic-sandwich echo sequences have been applied in a low-field NMR spectrometer [58]. This kind of pulse sequence provides near-quantitative refocusing of the rigid contribution to the initial part of proton free induction decay [58], allowing for a more quantitative determination of crystallinity in these gels. The results so obtained essentially confirm those shown in Fig. 10.

3.4 Structure of PVA Cryogels at Different Length Scales

The three-phase model adopted to describe the fraction of crystalline PVA in freeze–thaw hydrogels from X-ray diffraction analysis is in agreement with numerous studies.

For instance, in 1986, Yokoyama et al. investigated the morphology and structure of PVA freeze–thaw hydrogels (5–15 wt% of PVA), using a variety of techniques including X-ray diffraction, scanning electronic microscopy (SEM), and light optical microscopy [49]. They showed, by SEM analysis, that these gels have a porous structure, where the pore size increases from approximately 1 to 10 μm as the polymer concentration decreases from 15 to 5 wt%. They proposed a three-phase model to describe the porous structure of these gels (Fig. 11). The model consists of a water phase with a very low PVA concentration, an amorphous phase in which each PVA chain is swollen by water, and a PVA crystalline phase that partially prevents the motions of the amorphous chains. According to this model, the pores are mainly occupied by a polymer-poor phase that forms an interconnected continuous network, meandering through polymer-rich regions. The ice crystals are accommodated in the polymer-poor phase during the freezing step. The polymer-rich regions, in turn, are interconnected and build up the 3D network scaffold of the gels delimiting the pores. These regions consist of a swollen amorphous phase and PVA crystallites where the amorphous portions of chains connect the crystalline domains acting as junctions. Formation of the crystalline crosslinks ensures high dimensional stability and gives elastic properties to these gels.

The porous structure of PVA hydrogels is already imprinted in the first freeze–thaw cycle. This was shown by Fergg et al., using confocal laser scanning microscopy (CLSM) in the fluorescent mode [59], in the case of PVA hydrogels obtained by imposing a single freeze–thaw cycle (−15 °C for 24 h, then room temperature for 3 h). The advantage of using CLSM is that water does not need to be removed from hydrogels prior to examination. In the case of SEM analysis, dehydration procedures are always required before performing the observations, with the consequent drawback that the native morphology of gels might be significantly altered. Selected CLSM micrographs (extracted from [59]) of PVA hydrogels are shown in Fig. 12.

The pore or mesh size in these cryogels increases from ≈2 to 7 μm with decreasing PVA concentration. The CLSM analysis also indicates a tight interconnection of the pores all over the macroscopic samples, a uniform size of pores in the bulk, and no preferential structural orientation [59].

The complex architecture of PVA hydrogels, which includes a polymer-poor phase filling the pores and interconnected polymer-rich regions building the 3D network, made up by crystalline crosslinks connected by PVA chains belonging to the swollen amorphous regions (Fig. 11), has also been confirmed by small angle neutron scattering (SANS) measurements. Typical SANS profiles from as-formed PVA hydrogels obtained by subjecting a deuterated water solution of 11 wt% PVA

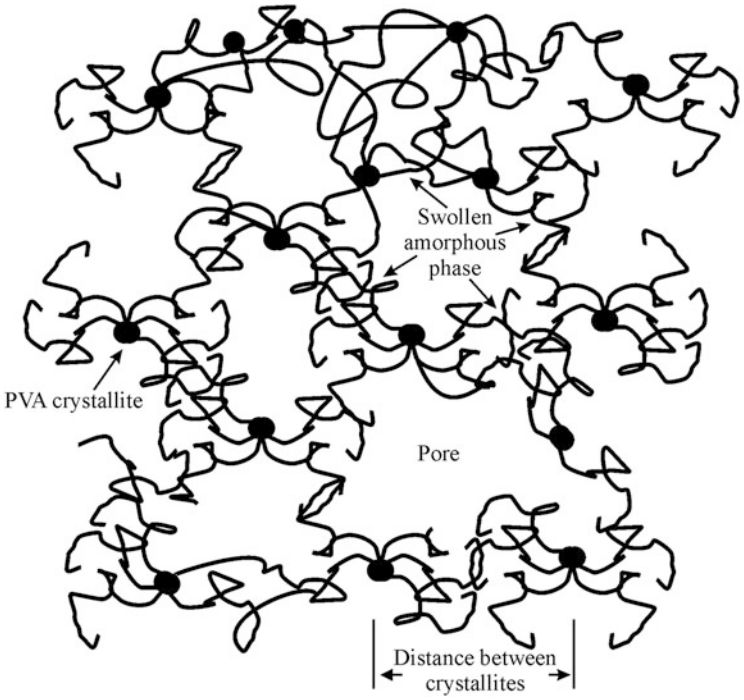

Fig. 11 Structural model of the porous structure for PVA hydrogels prepared by repeated freezing and thawing cycles [49]

to one (GEL-1) and nine (GEL-9) consecutive freeze–thaw cycles (20 h at −22 °C, then 4 h at 25 °C) are shown in Fig. 13 [60]. The SANS profile of the initial homogeneous solution is also shown in Fig. 13a.

It is apparent that the scattering cross-section profile $(d\sigma/d\Omega)$ from the homogeneous PVA solution denotes the presence of small scattering objects, essentially corresponding to individual chains of PVA with a Gaussian coil conformation (Fig. 13a). This curve is different from those of PVA GEL-*n* samples, indicating that PVA chains and solvent molecules are highly organized in these gels. In the SANS profiles of the gels, three different regions can be distinguished:

1. A region at low q values ($q < 0.09\ \text{nm}^{-1}$), where $q = 4\pi/(\lambda \sin\theta)$. In this region, the scattering cross-section exhibits an upturn, which is not present in the SANS curve of the initial homogeneous solution. In this zone, the data reflect a supramolecular organization, which has been associated with the presence of two separated phases constituted of polymer-rich and polymer-poor regions.
2. A region at intermediate q values ($0.09 < q < 0.35\ \text{nm}^{-1}$). In this region, an inflexion point is present at q^*, which gives the average distance L between the scattering crystallites, where $L \approx {}^{2\pi}/_{q^*}$. In all gel samples, this inflexion point

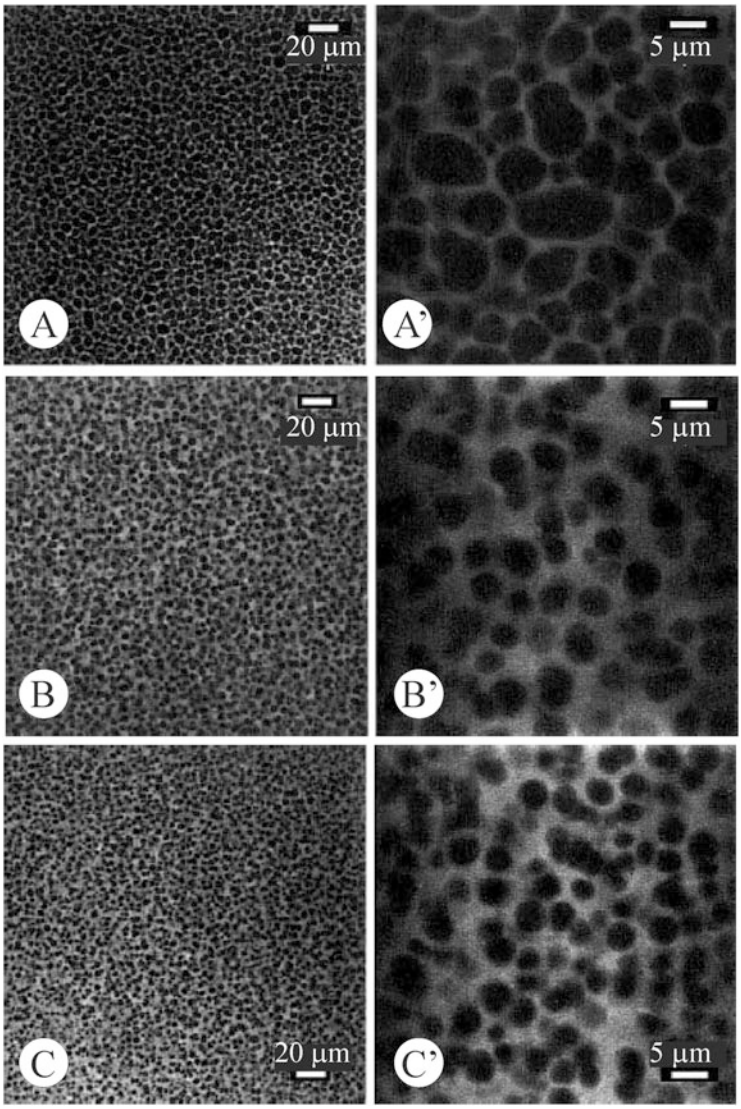

Fig. 12 (**a**–**c**′) Confocal laser scanning microscopy (CLSM) images of PVA hydrogels obtained by imposing a single freeze–thaw cycle on initial water solutions of PVA containing poly(ethylene glycol) PEG-600 of weight composition PVA/PEG/water 8/10/90 (**a**, **a**′), 12/10/90 (**b**, **b**′), and 16/10/90 (**c**, **c**′). All samples were examined after washing out PEG-600 and after addition of 5-dichlorotriazine fluorescein as fluorochrome. Images of bulk structures were taken at 10 μm (**a**, **a**′) and 15 μm under the surface (**b**, **b**′, **c**, **c**′) at two different magnifications as indicated [59]. (Reproduced with permission from [59]. Copyright 2001 by Springer)

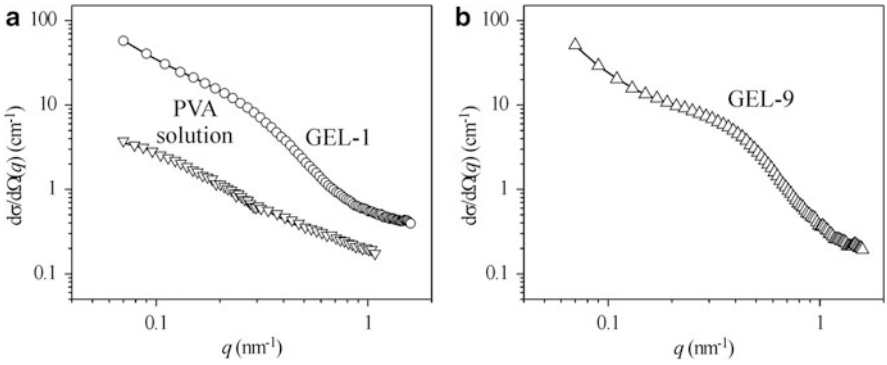

Fig. 13 SANS data from freshly prepared PVA cryogels (samples GEL-*n*) obtained by subjecting a deuterated water solution of 11 wt% PVA to (**a**) one (GEL-1) and (**b**) nine (GEL-9) consecutive freeze–thaw cycles (20 h at −22 °C, followed by 4 h at 25 °C). Data from the initial PVA solution (▽) used for gel preparation are included in **a**. $d\sigma/d\Omega$ is the scattering cross-section and q is the scattering vector, where $q = 4\pi/(\lambda \sin\theta)$, with θ being one half of the scattering angle. (Reproduced with permission from [60]. Copyright 2002 by the American Chemical Society)

occurs at $q^* \approx 0.03$ nm^{-1}, indicating a distance between crystallites of the order of 20 nm.

3. A region where $0.35 < q < 0.8$ nm^{-1}. In this zone, the scattering cross-sections decrease with a power law $d\sigma/d\Omega \propto q^{-D}$, where the value of D depends on the number of cycles. More precisely, $D \approx 2$ for GEL-1 and $D \approx 3$ for GEL-9. Provided we are looking in this region at the boundary structure between two phases, possibly the crystallites and the swollen amorphous phase, we may apply the surface fractal concept to the function $d\sigma/d\Omega$. According to this concept, the exponent D is related to the surface fractal dimension d_s in a d-dimensional space, through $D = 2d - d_s$. For example, in 3D space, d_s ranges from 2 to 3, corresponding to a range of D from 4 to 3. If the boundary were smooth, Porod's law $\left(d\sigma/d\Omega \propto q^{-4}\right)$ would be observed. For our PVA gels, values of D less than 4 suggest that the boundary is not smooth, due to some degree of interpenetration between the amorphous and crystalline phases at the interface.

From the analysis of SANS data [60], an average size of PVA crystallites equal to about 3 nm could be established, in good agreement with the coherence length of crystallites determined from the width at mid-height of $10\overline{1}$ reflection in the X-ray diffraction profiles of these gels (Fig. 9) by applying the Scherrer formula [42].

The hierarchical structural model emerging from microscopic, WAXS, and SANS investigations of PVA cryogels is shown in Fig. 14.

According to this model, PVA chains and solvent molecules in these gels are organized over different hierarchical length scales. At the micrometer length scale, two bi-continuous phases meandering around each other co-exist, consisting of

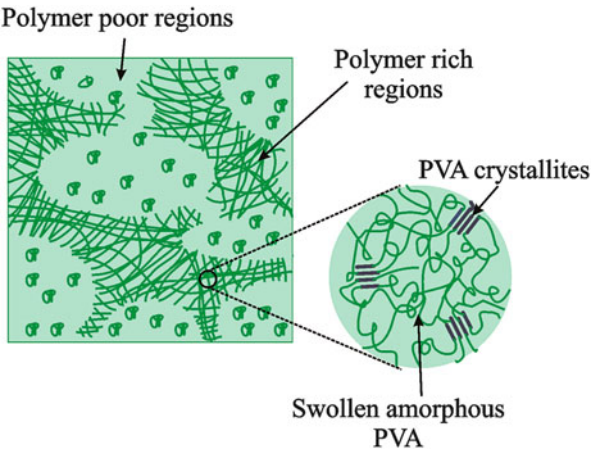

Fig. 14 The bi-continuous structure of PVA hydrogels obtained by freeze–thaw cycles with a PVA-rich phase and a PVA-poor phase. The fine structure of the polymer-rich region, including PVA crystallites and a swollen phase, is also indicated

polymer-rich and polymer-poor regions [4–6, 60, 61]. The polymer-rich regions (of average dimensions on the order of micrometers) [60] include crystallites of PVA of size equal to 3–4 nm [42, 60] and a swollen amorphous phase. The average distance between crystallites is on the order of 10–20 nm [60]. The polymer-poor regions, in turn, constitute the macropores and have sizes on the order of 1–10 μm [1, 4–6, 62, 63]. The physical crosslinks of the macroscopic network are essentially PVA crystallites connected by portions of chains swollen by the solvent [42, 57, 61].

3.5 Influence of Addition of Other Solvents

The influence of additional solvents to PVA/water solutions in the preparation of PVA gels by the freeze–thaw technique has been studied by numerous authors.

As an example, Hyon and Ikada prepared transparent hydrogels from PVA solutions in mixed solvents of water and water-miscible organic compounds [1, 64] such as dimethyl sulfoxide, glycerine, ethylene glycol, propylene glycol, and ethyl alcohol. Upon cooling these solutions to subzero temperatures, the presence of the organic solvent mixed with water prevents the PVA solution from freezing. At these temperatures PVA crystallization takes place, giving rise to formation of gels. The successive extraction of the organic solvent from the gels by exchange with water provides fully hydrated gels of PVA with high tensile strength, high water uptake, and high light transmittance. The last property is very important, especially for contact lenses applications [65]. The mechanism of gelation and formation of gels with increased light transmittance was explained as follows [64]: As the homogeneous solution is cooled, molecular motions are constrained. The consequence is that the interchain interactions of PVA, probably due to hydrogen

bonds, are promoted to yield small crystalline nuclei. Crystallization can proceed further as the solution remains at low temperatures for longer times. The crystallites serve as crosslinks to hold the 3D network structure. By addition of organic solvent, the PVA solution is prevented from freezing, even at temperatures below 0 °C. This permits PVA crystallization to proceed without a significant volume expansion. Therefore, the resulting gel contains pores smaller than 3 μm, giving rise to a transparent gel [1, 64].

In the case of PVA gels prepared by freezing and thawing techniques in the presence of ethylene glycol, Berghmans et al. suggested a two-step mechanism [66] involving a liquid–liquid phase separation in the first step (evidenced from the fact that the gel becomes opaque) followed by PVA crystallization in the polymer-rich phase in the second step.

Extensive studies have also been performed on PVA gels using mixtures of dimethyl sulfoxide and water as solvent (60/40 v/v) [67–73]. It was shown that gels prepared by freezing below –20 °C are transparent. Their properties depend on the ratio of dimethyl sulfoxide to water. It was also noted that gelation occurs below –20 °C without phase separation. However, above this temperature, LL phase separation plays an important role for the gelation process, giving rise to opaque gels.

Kanaya et al. used wide and small angle neutron scattering and light scattering experiments to provide extensive information concerning the structural organization of PVA gels formed in mixtures of DMSO and water at various length scales [67–73]. The presence of small PVA crystallites acting as crosslinks for the 3D network of these gels was confirmed. The crystallites have a sharp surface, presenting an average size of ≈7 nm and average distance of about 15–20 nm.

Trieu and Qutubuddin also investigated the structure of freeze–thaw PVA gels obtained from aqueous DMSO solutions [74, 75]. The authors characterized the gels by using freeze-etching and critical point drying SEM techniques. A higher porosity was observed at the surface than in the bulk of the gel.

It is worth noting that, regardless of the kind of solvent (pure water and/or water mixtures with other solvents), features common to PVA gels obtained by cryotropic treatments are the presence of a complex porous architecture that includes macropores filled with a polymer-poor phase and meandering polymer-rich regions. The tight interconnection of these pores allows for almost unhindered diffusion of large and small molecules [1, 4–6, 62, 63]. The polymer-rich regions are interconnected and constitute a biphasic 3D network consisting of a swollen amorphous PVA phase and PVA crystallites (Fig. 14). In all cases, although hydrogen bond interactions play a key role in creating the physical junctions of the network, the high dimensional stability and mechanical strength achieved by these gels is due to the presence of crystalline crosslinks. In particular, the size and amount of PVA crystalline aggregates in freeze–thaw PVA hydrogels play important roles in gel performance because the dimensional stability, toughness, strength to external stresses, and thermal stability of PVA cryogels are critically dependent on these parameters.

3.6 Mechanism of Formation of PVA Cryogels

The mechanism of formation of the hierarchical structure of PVA cryogels featuring an open porous structure is the result of the occurrence of at least three concomitant and, at the same time, conflicting processes: crystallization of the solvent, LL phase separation, and crystallization of PVA. At subzero temperatures, solutions having the typical concentrations used for preparation of PVA cryogels are below the spinodal curve shown in Fig. 8 [4–6, 43]. Therefore, during freezing and successive permanence of the solution at subzero temperatures, a LL phase separation may occur in addition to the crystallization of solvent and PVA. The exact mechanism of formation of the macroporous structure (i.e., water crystallization at subzero temperatures or LL phase separation, or the concomitant effect of both transitions) depends on a number of factors such as the cooling rate at subzero temperatures, the use of other solvents mixed with water, the presence of additives, and the PVA concentration [4–6].

Applying the arguments given in Sect. 2, the formation mechanism of PVA cryogels represents a paradigmatic example of the Ostwald "stage rule" [17, 25, 33]. This means that, upon formation of these gels, a hierarchy of metastability may arise due to the possible occurrence of several metastable phases via different processes [17, 25]. Therefore, when a given process is arrested by an agency before completion, the system is frozen in a phase of circumstantial metastability that, once formed, has the potential to evolve faster than the transition leading to the ultimate stable phase and may dominate the whole transformation process [17, 25].

Lozinsky and coworkers [4–6] suggested a general mechanism for cryotropic gelation, which is illustrated in Fig. 15.

In this model, the initial solution (Fig. 15a), is frozen at temperatures slightly below the solvent crystallization point, giving rise to an inhomogeneous system that includes an unfrozen liquid microphase along with crystals of the frozen solvent (Fig. 15b). Since the polymer (and any other additive) are generally rejected in the unfrozen liquid microphase, the solute concentration in the unfrozen liquid microphase is higher than in the initial solution. At this stage, a crosslinking process (chemical or physical) may easily take place in the unfrozen liquid microphase, leading to the formation of microgel fractions. If the regions occupied by the microgel fraction achieve an interconnected structure, a macroscopic gel is obtained upon defrosting. Thus, Lozinsky considered that cryogels are formed inside these unfrozen microregions of the frozen system [4–6]. During freezing, the crystals of frozen solvent act as a porogen and grow until they meet the facets of other solvent crystals. Upon thawing, the system transforms into a macroporous cryogel containing large interconnected pores with variable size and geometry (Fig. 15c). The dimensions and shape of the pores are related to the volume of the unfrozen liquid microphase, which depends on numerous factors such as the nature of solvent, initial polymer concentration, the molecular weight of solutes, the system temperature, and the presence of soluble or insoluble admixtures [4–6].

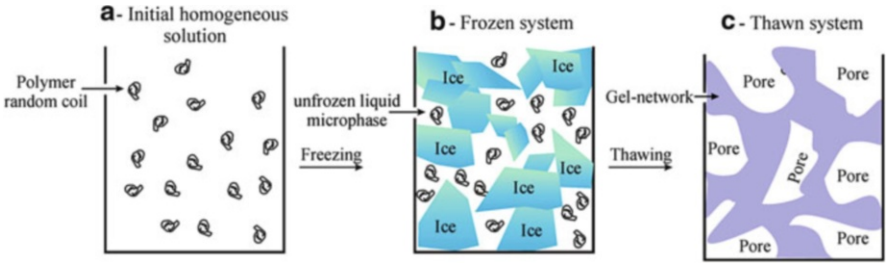

Fig. 15 Mechanism for cryotropic gelation according to the model suggested by Lozinsky [4–6]. During (**a**) freezing of an initially homogeneous solution, incomplete solvent crystallization occurs, leading to (**b**) the formation of an unfrozen liquid microphase. Gelation takes place in these unfrozen regions, forming a microgel fraction. (**c**) Upon defrosting, the regions occupied by solvent crystals give rise to the pores, whereas the regions occupied by the microgel fraction may achieve an interconnected structure that gives rise to the macroscopic 3D network of the gels

Based on data obtained by cryogenic transmission electron microscopy (cryo-TEM), solid-state NMR, X-ray scattering, and DSC, Willcox et al. [61] proposed a model for PVA cryogels similar to that proposed by Yokoyama (Fig. 11) [49]. In particular, they showed that during the first freeze–thaw cycle a few small crystallites are formed (with size of about 3–8 nm), which are connected in an irregular porous network by amorphous chains highly swollen by the solvent. They found that the average crystal–crystal distance (mesh size) is ≈30 nm. Upon aging these gels, or by subjecting them to a second freeze–thaw cycle, the level of crystallinity increases, whereas the crystallite size and the mesh size remain nearly constant. This suggests that the formation of secondary crystallites does not affect the network connectivity. Cryo-TEM observation of these gels essentially confirmed the presence of pores located at the same mesh distance as crystallites [61]. Therefore, Willcox and colleagues [61] point out the existence of pores sized one order of magnitude lower than the macropores visualized in other investigations [49, 59] (Fig. 12). We infer that these pores are formed inside the polymer-rich regions and coexist with the macropores. The possible mechanism of formation of these gels, involving dendritic ice crystallization and possibly spinodal decomposition, are also discussed [61].

Our group has used TR-SANS to perform extensive investigations on the cryotropic gelation of PVA/D_2O solutions during consecutive freeze–thaw cycles [76, 77]. Measurements have been performed on solutions of 5.03, 10.11, and 14.22 wt% PVA, corresponding to PVA volume fractions Φ of 0.042, 0.086, and 0.12, respectively. In Fig. 16a, the SANS data collected during the freezing (at –13 °C) and thawing (at 20 °C) steps are shown for a solution with PVA volume fraction $\Phi = 0.086$ [76, 77] as an example.

The scattering cross-section increases during freezing (Fig. 16a). This increase is essentially due to structural changes associated with the crystallization of the water in the solution. Nearly constant values are achieved for the frozen solution after 30 min at −13 °C (curve d in Fig. 16a). The presence of a knee at

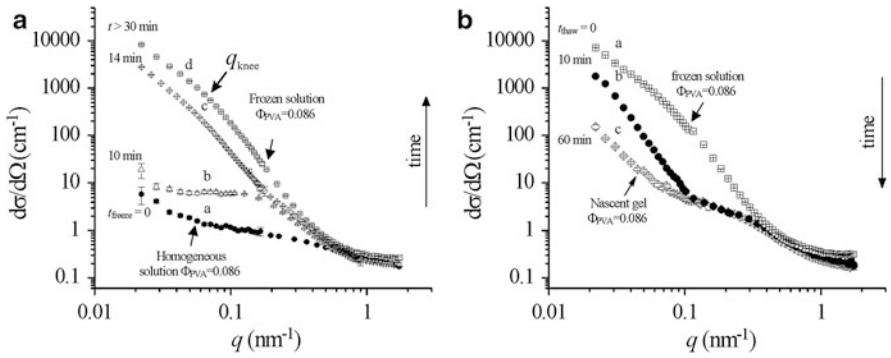

Fig. 16 Change in the scattering cross-section as a function of the scattering vector q: (**a**) from an initial solution with $\Phi_{PVA} = 0.086$, collected at room temperature ($t_{freeze} = 0$) (*a*) and after successive freezing and permanence of the solution at −13 °C for 10 min (*b*), 14 min (*c*), and 30 min (*d*); and (**b**) from the frozen solution after 390 min at −13 °C ($t_{thaw} = 0$) (*a*) and after successive thawing and permanence at 20 °C for 10 min (*b*) and 60 min (*c*). (Reproduced with permission from [77]. Copyright 2008 by the American Chemical Society)

$q_{knee} \approx 0.07$ nm^{-1}, with a power law dependence of the scattering cross-section as $d\sigma/d\Omega \approx q^{-2.2}$ for $q < q_{knee}$ and as $d\sigma/d\Omega \approx q^{-3.7}$ for $q > q_{knee}$ (curve d in Fig. 16a), indicates that the frozen system includes heterogeneities within the ice matrix, corresponding to the unfrozen liquid microphase [76, 77] of characteristic size $L = 2\pi/q_{knee} \approx 75$–80 nm. The above analysis also indicates that the unfrozen liquid microphase is organized to form fractal aggregates of dimensions above 300 nm within the ice matrix. This scenario is in agreement with the mechanism for cryotropic gelation suggested by Lozinsky [4–6] (Fig. 15).

The solutions with PVA content $\Phi = 0.086$, and 0.12 form a gel upon defrosting after 390 min at −13 °C (curve c of Fig. 16b). However, the solution with $\Phi = 0.042$ is unable to jellify upon the same cryotropic treatment [77]. This indicates that for polymer concentrations below a critical value, the total volume of the unfrozen liquid microphase is too low to form cluster aggregates [77]. The clustering process, in turn, plays a key role in formation of the gel.

It is worth noting that the analysis of SANS data in Fig. 16a, related to the early stages of cryogelation from PVA homogeneous solutions, does not provide any evidence of LL phase separation during the prolonged treatment at subzero temperatures, as expected from the phase diagram of Komatsu et al. [43] (Fig. 8). In fact, the fastest process that could be detected in our approach is crystallization of the solvent [76, 77]. Using the concept of hierarchical metastability [17, 25], this occurs because the spinodal decomposition is buried by the crystallization of water. In this hypothesis and in agreement with the cryogelation mechanism proposed by Lozinsky [4–6] (Fig. 15), the formation of macropores in these gels is due to crystallization of the solvent, which acts as a porogen. However, the lack of evidence of LL phase separation may also be due to the fact that in the early stages of spinodal decomposition, concentration fluctuation corresponds to wavelengths

higher than $2\pi/q_{min}$ (≈300 nm) [24, 37, 78], with $q_{min} = 0.02$ nm^{-1} being the lowest value of the scattering vector q that was achieved in the experimental set-up. In this second hypothesis, the scattering intensity is expected to show a peak at $q < q_{min}$, but this low q region was not sampled [24, 37].

During thawing, the scattering cross-section decreases (Fig. 16b). This indicates that, upon defrosting, the frozen solution evolves towards a system characterized by alternation of dense and diluted regions that have origin in the regions occupied at subzero temperatures by ice and the unfrozen liquid microphase, respectively [77]. For PVA concentrations higher than a critical value, dense and diluted regions are likely to form an interpenetrated network of two co-continuous phases, resulting in a transparent gel in the nascent state (curve c of Fig. 16b) where the characteristic size of the phase-separated domains is of the order of few tens of nanometers [77].

The nascent gels become opaque upon aging at room temperature for few hours due to the increase in size of the regions that are alternatively dense and diluted [77]. The coarsening of the heterogeneous structure imprinted by the cryotropic treatment is driven by the tendency of the dense and dilute regions to minimize their surface of contact, and is the hallmark that these gels are in a state far from equilibrium. In fact, the fast cryogenic treatment causes the formation of transparent gels having the same composition as the initial homogeneous solution. On the basis of the phase diagram by Komatsu et al. [43] (Fig. 8), solutions containing 10–12 wt% PVA (corresponding to PVA volume fraction Φ in the range 0.086–0.12) are in the one-phase region and should not give rise to a gel at room temperature. However, the nascent gels obtained from these solutions by cryotropic treatment at −13 °C do not transform back into the initial homogeneous solution once they are brought back to room temperature because a strong network scaffolding has already been formed due to the presence of PVA crystallites. These gels are stable up to 50–60 °C [57] and can be aged for long time in sealed vials, maintaining their properties. Moreover, the nascent gels obtained after a single freeze–thaw cycle are already too strong to evolve towards complete elimination of the solvent [24]. Nascent gels, instead, react via microsyneresis and the size of the dense and diluted regions increases [24]. The coarsening of the heterogeneous structure of the nascent and transparent gels, up to becoming opaque, also suggests that spinodal decomposition occurs [79, 80]. This phenomenon has indeed been observed for other gels [79, 80]. It generally occurs when a swollen gel is suddenly brought into another state that may be located either in the two-phase or one-phase region of its phase diagram [80]. Regardless of the region of the phase diagram in which the new state is located, it has been shown that the system becomes opaque without any appreciable volume change, suggesting occurrence of spinodal decomposition in both cases. However, in contrast to the usual fluids, the domain growth is slow because the elastic force of the gel suppresses the surface tension force, which is the driving force of domain growth [79, 80].

3.7 Kinetic Analysis of SANS Data

A more in-depth analysis of TR-SANS data collected during the first freezing step (Fig. 16a) indicates that the structural changes that occur at correlation distances between 60–300 nm and 7–60 nm are different and involve different characteristic times [77]. Therefore, the scattering data collected in the relevant q ranges were analyzed separately by evaluating the Lorentz-corrected integral Ψ of the scattering cross-section in the q range between $q_1 = 0.022$ and $q_2 = 0.108$ nm^{-1} for $\Psi_{low}(t)$ and between $q_1 = 0.108$ and $q_2 = 0.881$ nm^{-1} for $\Psi_{high}(t)$ as a function of time. This kind of integral corresponds to the scattering invariant when the integration limits in q are extended from zero to infinite. For this reason, the function Ψ corresponds to a sort of "reduced scattering invariant." A working hypothesis is that, in the early stages of gelation, the SANS patterns contain additive contributions from the aggregated and non-aggregated phases and that the interaction between these two phases may be neglected. Thus, changes in the reduced scattering invariant $\Psi_{low}(t)$ probe structural changes occurring in the initially homogeneous solution during permanence at subzero temperatures at length scales of the order of hundreds of nanometers, essentially due to water crystallization [77]. By contrast, changes in the reduced scattering invariant $\Psi_{high}(t)$ probe structural changes occurring at length scales of the order of nanometers, essentially due to PVA crystallization inside the unfrozen liquid microphase [77].

The values of the reduced scattering invariant calculated from the SANS data collected during the first freezing step of PVA/D_2O solutions are reported in Fig. 17 as a function of the permanence time of the solutions at −13 °C. In Fig. 17a′ (inset), the values of $\Psi_{low}(t)$ of pure D_2O are also shown for comparison.

The sigma shape of the curves describing the structural changes occurring at a length scale of hundreds of nanometers (Fig. 17a) reflects the formation of ice crystals of pure water (Fig. 17a′), which takes about 10–15 min regardless of PVA concentration [77].

By contrast, the values of the reduced scattering invariant calculated in the high q region $\Psi_{high}(t)$ increase with the permanence time of the PVA solutions at subzero temperature according to a smoothed sigma shape (Fig. 17b), and reflect structural changes at length scales of tens of nanometers due to the crystallization of PVA in the unfrozen liquid microphase. It is apparent that the values of $\Psi_{high}(t)$, regardless of PVA concentration, increase smoothly in the first 30 min, present an upturn at around 30–40 min, and increase smoothly again in the successive 120–330 min of freezing, without reaching any plateau value, even for prolonged times of permanence at −13 °C. This suggests that after completion of the crystallization of the solvent (which takes about 10–15 min), the PVA chains, which are mostly segregated in the unfrozen liquid microphase, tend to form precrystalline or crystalline aggregates, probably because the concentration of the liquid microphase reaches the eutectic composition [77]. However, although the temperature of the system (−13 °C) is probably below the eutectic temperature, the full crystallization of PVA may not be achieved and is slowed down due to the fact that the unfrozen liquid

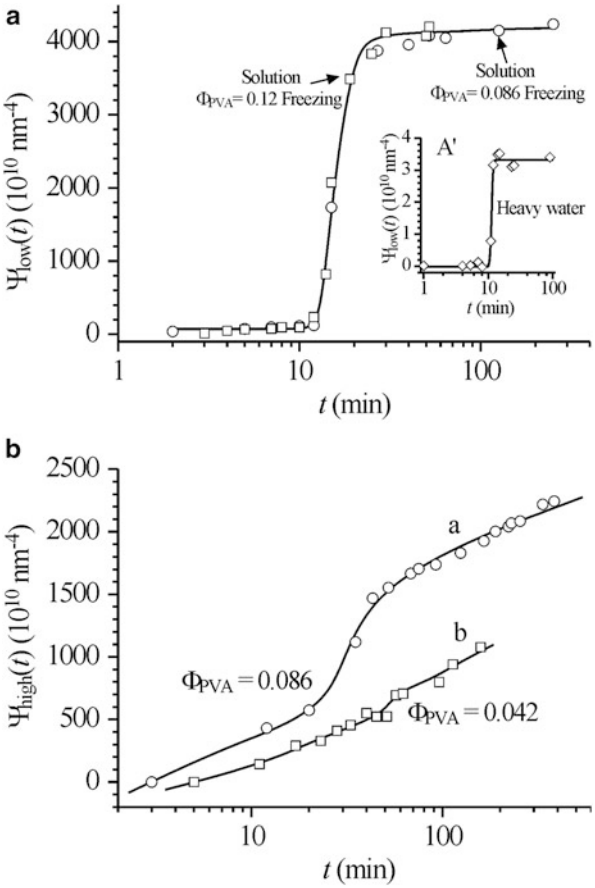

Fig. 17 (**a**, **a**′) Reduced scattering invariant, $\Psi_{low}(t)$, as a function of time during treatment at –13 °C from a D_2O solution with $\Phi_{PVA} = 0.086$ (*circles*) and 0.12 (*squares*) PVA volume fraction (**a**) and from pure D_2O (**a**′, *inset*). The *curves* reflect structural changes occurring at length scales of the order of hundreds of nanometers, essentially due to water crystallization. (**b**) Reduced scattering invariant, $\Psi_{high}(t)$, as a function of time during the treatment at –13 °C from a D_2O solution with 0.086 (*curve a*) and 0.042 (*curve b*) PVA volume fraction. The *curves* reflect structural changes occurring at length scales of the order of nanometers, essentially due to PVA crystallization inside the unfrozen liquid microphase. (Reproduced with permission from [77]. Copyright 2008 by the American Chemical Society)

microphase jellifies, preventing attainment of thermodynamic equilibrium [77]. The formation of the gel microphase may be determined by aggregation of PVA chains in a confined environment, which is driven by hydrogen bonding, consequent formation of crystallites, and vitrification of the swollen amorphous phase at a temperature that is probably below the glass transition [4–6]. This scenario holds both for solutions with PVA volume fraction $\Phi \geq 0.086$ and for

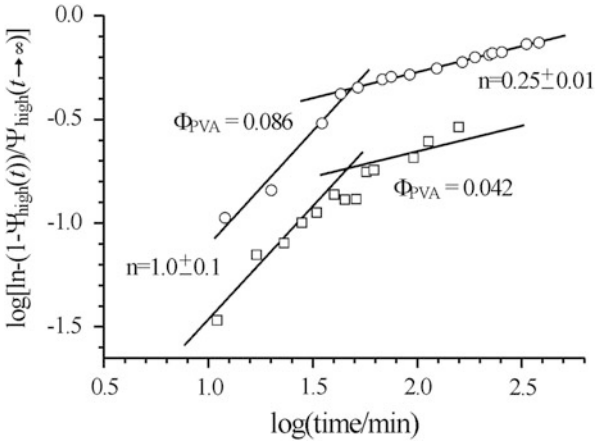

Fig. 18 Avrami plot of the reduced scattering invariant $\Psi_{high}(t)$ normalized to the extrapolated value of the scattering invariant at infinite time $\Psi_{high}(t \rightarrow \infty)$ for solutions with PVA volume fraction Φ_{PVA} of 0.086 (*circles*) and 0.042 (*squares*). The Avrami exponents n are indicated. (Reproduced with permission from [77]. Copyright 2008 by the American Chemical Society)

more dilute PVA solutions with $\Phi = 0.042$ (curve b of Fig. 17b). In fact, the SANS data in Fig. 17b indicate that in dilute PVA solution ($\Phi = 0.042$), crystallization of PVA probably also takes place, even though a macroscopic gel is not formed upon defrosting because the relative amount of the gel microphase is too low to give rise to an interconnected macroscopic gel network at subzero temperatures [77].

The data in Fig. 17b may be used to extrapolate the value of the reduced scattering invariant $\Psi_{high}(t)$ at infinite time $\Psi_{high}(t \rightarrow \infty)$ [77]. The ratio of $\Psi_{high}(t)$ to $\Psi_{high}(t \rightarrow \infty)$ is proportional to the extent of PVA crystallization in the unfrozen liquid microphase. This parameter is used in the Avrami plot shown in Fig. 18 [77]. Avrami analysis of the confined crystallization in these gels indicates that the confined crystallization of PVA follows first-order kinetics ($n = 1$) during the first 40 min, and becomes slower in the later stages with an apparent exponent $n < 1$ [77]. For the frozen solution, an exponent of $n \approx 1$ is consistent with a one-dimensional (fibrillar) growth mechanism controlled by heterogeneous (athermal) nucleation [81], triggered by the active surface of ice at the interface with the unfrozen liquid microphase. The low Avrami exponent of 0.25 is rather uncommon [82, 83]. A possible reason for a value of n lower than 1 in the later stages of crystallization kinetics of PVA in the frozen solution may be the restriction of crystal growth because previously formed PVA crystals reduce the mobility of PVA chains dissolved in the unfrozen liquid microphase. This reduced mobility, in turn, results in jellification of the unfrozen microphase [77].

4 Concluding Remarks and Outlook

Poly(vinyl alcohol) cryogels are strong physical gels that form as a result of different crosslinking processes that occur simultaneously in synergy or in competition. We demonstrate here that the concept of circumstantial metastability and the hierarchy of metastable states may turn out to be useful in unraveling the complex mechanisms subtending their formation. In particular, we have shown that kinetic analysis of the cryotropic gelation from PVA solutions using time-resolving SANS has allowed an unprecedented level of comprehension of this process. At least three elementary steps have been identified:

- Incomplete solvent crystallization occurring at subzero temperatures, with consequent formation of an unfrozen liquid microphase of eutectic composition
- Incomplete PVA crystallization in the unfrozen liquid microphase, with consequent formation of a microgel fraction
- Coarsening of the dense and diluted regions imprinted by the cryogenic treatment, occurring at room temperature

A wealth of applications have been proposed for these gels in many different fields, including biomedicine and diagnostics. Applications include the building of artificial muscles [84, 85] or phantom organs for NMR imaging and mammography [86, 87], controlled drug release [11, 88–90], and biotechnology in which these gels act as carriers of immobilized bioaffinity ligands, enzymes, and cells [4–6, 91].

More recently, it has been pointed out that aged gels possess self-healing properties at room temperature, without the need for any stimulus or healing agent [10]. Welding occurs spontaneously via chain diffusion across the interface provided that a sufficient number of PVA free hydroxyl groups survive at the contact between the two cut surfaces [10].

A further interesting property of PVA cryogels is that, whereas a long aging in sealed vials at room temperature induces large variations in their structure and properties, the porous structure imprinted by cryotropic treatment is not greatly altered upon drying and during the successive rehydration step. Rehydrated gels almost completely recover the volume, shape, and physical properties of the as-formed freeze–thaw PVA hydrogels [42, 57, 62, 63]. It has been shown that the outstanding physical and mechanical properties of freeze–thaw PVA hydrogels in the as-prepared state can be preserved, even for a long time, by drying the samples immediately after preparation and then restoring when needed by rehydration of the dried samples [42, 57, 63].

Finally, it is worth mentioning that PVA cryogels are able to incorporate different soluble and insoluble additives inside the pores to obtain composite materials of both scientific and applied interest [4–6]. In particular, PVA-based cryogels have been obtained that include inside the porous structure nanoparticles of solid crystalline compounds, co-elastic gels, microorganisms, gas bubbles, or microdroplets of liquids immiscible with PVA solutions [4–6, 92–98].

There are still several basic issues regarding PVA cryogels that deserve further investigation, especially related to the complex dynamics of water molecules and polymer chains. The identification of smart processing routes to obtain systems with tailored pore size and pore size distribution, and with well-defined viscoelastic properties, is critically dependent on fundamental study of the dynamics of these systems, coupled with modeling.

References

1. Hassan CM, Peppas NA (2000) Structure and applications of poly(vinyl alcohol) hydrogels produced by conventional crosslinking or by freezing/thawing methods. Adv Polym Sci 153:37
2. Peppas NM (1975) Turbidimetric studies of aqueous poly(vinyl alcohol) solutions. Makromol Chem 176:3433
3. Stauffer S, Peppas NA (1992) Poly(vinyl alcohol) hydrogels prepared by freezing-thawing cyclic processing. Polymer 33:3932
4. Lozinsky VI (1998) Cryotropic gelation of poly(vinyl alcohol) solutions. Russ Chem Rev 67:573
5. Lozinsky VI (2002) Cryogels on the basis of natural and synthetic polymers: preparation, properties and application. Russ Chem Rev 71:489
6. Lozinsky VI, Galaev IY, Plieva FM, Savina IN, Jungvid H, Mattiasson B (2003) Polymeric cryogels as promising materials of biotechnological interest. Trends Biotechnol 21:445
7. Lozinsky VI, Damshkaln LG (2000) Study of cryostructuration of polymer systems. XVII. Poly(vinyl alcohol) cryogels: dynamics of the cryotropic gel formation. J Appl Polym Sci 77:2017
8. Watase M, Nishinari K (1985) Reological and DSC changes in poly(vinyl alcohol) gels induced by immersion in water. J Polym Sci Part B: Polym Phys Ed 23:1803
9. Nishinari K, Watase M, Tanaka F (1996) Structure of junction zones in poly(vinyl alcohol) gels by rheological and thermal studies. J Chim Phys Phys Chim Biol 93:880
10. Zhang H, Xia H, Zhao Y (2012) Poly(vinyl alcohol) hydrogel can autonomously self-heal. ACS Macro Lett 1:1233
11. Peppas NA, Mongia NK (1997) Ultrapure poly(vinyl alcohol) hydrogels with mucoadhesive drug delivery characteristics. Eur J Pharm Biopharm 43:51
12. Finch CA (1992) Polyvinyl alcohol – developments. Wiley, London
13. Bolto B, Tran T, Hoang M, Xie Z (2009) Crosslinked poly(vinyl alcohol) membranes. Prog Polym Sci 34:969
14. Cohen Addad JP (1996) Physical properties of polymeric gels. Wiley, London
15. Loh XJ, Scherman OA (2013) Polymeric and self-assembled hydrogels. The Royal Society of Chemistry, Cambridge
16. Papon P, Leblond J, Meijer PHE (2002) The physics of phase transitions: concepts and applications. Springer, Berlin
17. Keller A (1995) Aspects of polymer gels. Faraday Discuss 101:1
18. Shibayama M, Tanaka T (1993) Volume phase transition and related phenomena of polymer gels. Adv Polym Sci 109:1
19. Rubinstein M, Colby RH (2003) Polymer physics. Oxford University Press, New York
20. Tanaka T (1981) Gels Sci Am 244:124
21. Tanaka T, Sun ST, Hirokawa Y, Katayama S, Kucera J, Hirose Y, Amiya T (1987) Mechanical instability of gels at the phase transition. Nature 325:796

22. Durmaz-Hilmioglu N, Yildirim AE, Sakaoglu AS, Tulbentci S (2001) Acetic acid dehydration by pervaporation. Chem Eng Proc 40:263
23. Benzekri K, Essamri A, Toreis N, Souissi A, Maarouf T, Mas A (2001) Membranes d'alcool polyvinylique traitées par plasma d'acide acrylique. Application à la déshydratation des mélanges eau–éthanol par pervaporation. Eur Polym J 37:1607
24. deGennes P-G (1979) Scaling concepts in polymer physics. Cornell University Press, Ithaca
25. Keller A, Cheng SZD (1998) The role of metastability in polymer phase transitions. Polymer 39:4461
26. Atkins EDT, Isaac DH, Keller A, Miyasaka K (1977) Analysis of anomalous X-ray diffraction effects of isotactic polystyrene gels and its implications for chain conformation and isomeric homogeneity. J Polym Sci Polym Phys Ed 15:211
27. Atkins EDT, Isaac DH, Keller A (1980) Conformation of polystyrene with special emphasis to the near all-trans extended-chain model relevant in polystyrene gel. J Polym Sci Polym Phys Ed 18:71
28. Atkins EDT, Keller A, Shapiro JS, Lemstra PJ (1981) Extended-chain structure for isotactic polystyrene: additional X-ray diffraction and calorimetric results. Polymer 22:1161
29. Girolamo M, Keller A, Miyasaka M, Overbergh N (1976) Gelation-crystallization in isotactic polystyrene solutions and its implications to crystal morphology, to the origin and structure of gels, and to the chemical homogeneity of polyolefins. J Polym Sci Polym Phys Ed 14:39
30. Chatani Y, Nakamura N (1993) Coiled-coil molecular model for isotactic polystyrene gels. Polymer 34:1644
31. Auriemma F, De Rosa C, Corradini P (2004) Non-helical chain conformations of isotactic polymers in the crystalline state. Macromol Chem Phys 205:390
32. Guenet J-M (1992) Thermoreversible gelation of polymers and biopolymers. Academic, London, 1992
33. Ostwald W (1897) Studies on the formation and inversion of solids. First paper: supersaturation and supercooling. Z Phys Chem 22:289
34. Hikmet RM, Callister S, Keller A (1988) Thermoreversible gelation of atactic polystyrene: phase transformation and morphology. Polymer 29:1378
35. Wellinghoff ST, Shaw J, Baer E (1979) Polymeric materials from the gel state. The development of fringed micelle structure in a glass. Macromolecules 12:932
36. Arnauts J, Berghmans H (1987) Amorphous thermoreversible gels of atactic polystyrene. Polym Commun 28:66
37. Strobl GR (2007) The physics of polymers. Springer, Berlin
38. Berghmans S, Mewis J, Berghmans H, Meijer H (1995) Phase behavior and structure formation in solutions of poly(2,6-dimethyl-1,4-phenylene ether). Polymer 36:3085
39. Tubbs RK (1966) Sequence distribution of partially hydrolyzed poly(vinyl acetate). J Polym Sci A1 4:623
40. Bunn CW, Peiser HS (1947) Mixed crystal formation in high polymers. Nature 159:161
41. Bunn CW (1948) Crystal structure of polyvinyl alcohol. Nature 161:929
42. Ricciardi R, Auriemma F, De Rosa C, Lauprêtre F (2004) X-ray diffraction analysis of poly (vinyl alcohol) hydrogels obtained by freezing and thawing techniques. Macromolecules 37:1921
43. Komatsu M, Inoue T, Miyasaka K (1986) Light-scattering studies on the sol–gel transition in aqueous solutions of poly(vinyl alcohol). J Polym Sci: Polym Phys Ed 24:303
44. Kawanishi K, Komatsu M, Inoue T (1987) Thermodynamic consideration of the sol-gel transition in polymer solutions. Polymer 28:980
45. Pines E, Prins W (1973) Structure-property relations of thermoreversible macromolecular hydrogels. Macromolecules 6:888
46. Peppas NA (1976) Crystallization of polyvinyl alcohol-water films by slow dehydration. Eur Polym J 12:495
47. Mallapragada SK, Peppas NA (1996) Dissolution mechanism of semicrystalline poly(vinyl alcohol) in water. J Polym Sci Part B: Polym Phys 34:1339

48. Kukharchik MM, Baramboim NK (1972) Change in the properties of aqueous solutions of poly (vinyl alcohol) during cryolytic action. Vysokomol Soedin 14B:843
49. Yokoyama F, Masada I, Shimamura K, Ikawa T, Monobe K (1986) Morphology and structure of highly elastic poly(vinyl alcohol) hydrogel prepared by repeated freezing-and-melting. Colloid Polym Sci 264:595
50. Watase M, Nishinari K (1989) Effect of the degree of saponification on the rheological and thermal properties of poly(vinyl alcohol) gels. Makromol Chem 190:155
51. Kobayashi M, Ando I, Ishii T, Amiya S (1995) Structural study of poly(vinyl alcohol) in the gel state by high-resolution solid-state ^{13}C NMR spectroscopy. Macromolecules 28:6677
52. Kobayashi M, Ando I, Ishii T, Amiya S (1998) Structural and dynamical studies of poly(vinyl alcohol) gels by high-resolution solid-state ^{13}C NMR spectroscopy. J Mol Struct 440:155
53. Kobayashi M, Kanekiyo M, Ando I (1998) A study of molecular motion of PVA/water system by high-pressure ^{1}H pulse-NMR method. Polym Gels Netw 6:347
54. Kanekiyo M, Kobayashi M, Ando I, Kurosu H, Ishii T, Amiya S (1998) A structural and dynamic study of poly(vinyl alcohol) in the gel state by solid-state ^{13}C NMR and ^{1}H pulse NMR. J Mol Struct 447:49
55. Terao T, Maeda S, Saika A (1983) High-resolution solid-state carbon-13 NMR of poly(vinyl alcohol): enhancement of tacticity splitting by intramolecular hydrogen bonds. Macromolecules 16:1535
56. Ricciardi R, Gaillet C, Ducouret G, Lafuma F, Lauprêtre F (2003) Investigation of the relationships between the chain organization and rheological properties of atactic poly(vinyl alcohol) hydrogels. Polymer 44:3375
57. Ricciardi R, Auriemma F, Gaillet C, De Rosa C, Lauprêtre F (2004) Investigation of the crystallinity of freeze/thaw poly(vinyl alcohol) hydrogels by different techniques. Macromolecules 37:9510
58. Valentín JL, López D, Hernández R, Mijangos C, Saalwächter K (2009) Structure of poly (vinyl alcohol) cryo-hydrogels as studied by proton low-field NMR spectroscopy. Macromolecules 42:263
59. Fergg F, Keil FJ, Quader H (2001) Investigations of the microscopic structure of poly(vinyl alcohol) hydrogels by confocal laser scanning microscopy. Colloid Polym Sci 279:61
60. Ricciardi R, Mangiapia G, Lo Celso F, Paduano L, Triolo R, Auriemma F, De Rosa C, Lauprêtre F (2005) Structural organization of poly(vinyl alcohol) hydrogels obtained by freezing and thawing techniques: a SANS study. Chem Mater 17:1183
61. Willcox PJ, Howie DW Jr, Schimdt-Rohr K, Hoagland A, Gido SP, Pudjijanto S, Kleiner LW, Venkatraman S (1999) Microstructure of poly(vinyl alcohol) hydrogels produced by freeze/thaw cycling. J Polym Sci Part B: Polym Phys 37:3438
62. Ricciardi R, D'Errico G, Auriemma F, Ducouret G, Tedeschi AM, De Rosa C, Lauprêtre F, Lafuma F (2005) Short time dynamics of solvent molecules and supramolecular organization of poly (vinyl alcohol) hydrogels obtained by freeze/thaw techniques. Macromolecules 38:6629
63. Tedeschi A, Auriemma F, Ricciardi R, Mangiapia G, Trifuoggi M, Franco L, De Rosa C, Heenan RK, Paduano L, D'Errico G (2006) A study of the microstructural and diffusion properties of poly(vinyl alcohol) cryogels containing surfactant supramolecular aggregates. J Phys Chem B 110:23031
64. Hyon S-H, Ikada Y (1987) Porous and transparent poly(vinyl alcohol) gel and method of manufacturing the same. US Patent 4663358
65. Hyon S-H, Cha W-I, Ikada Y, Kita M, Ogura Y, Honda Y (1994) Poly(vinyl alcohol) hydrogels as soft contact lens material. J Biomater Sci Polym Ed 5:397
66. Berghmans H, Stoks W (1986) Thermoreversible gelation of vinylpolymers. In: Kleintjens LA, Lemstra PJ (eds) Integration of fundamental polymer science and technology. Springer, London
67. Kanaya T, Ohkura M, Kaji H, Furusaka M, Misawa M (1994) Structure of poly(viny1 alcohol) gels studied by wide- and small-angle neutron scattering. Macromolecules 27:5609

68. Kanaya T, Takeshita H, Nishikoji Y, Ohkura M, Nishida K, Kaji K (1998) Micro- and mesoscopic structure of poly(vinyl alcohol) gels determined by neutron and light scattering. Supramol Sci 5:215
69. Kanaya T, Ohkura M, Takeshita H, Kaji H, Furusaka M, Yamaoka H, Wignall GD (1995) Gelation process of poly(viny1 alcohol) as studied by small-angle neutron and light scattering. Macromolecules 28:3168
70. Takeshita H, Kanaya T, Nishida K, Kaji K (2002) Small-angle neutron scattering studies on network structure of transparent and opaque PVA gels. Physica B 311:78
71. Takeshita H, Kanaya T, Nishida K, Kaji K (1999) Gelation process and phase separation of PVA solutions as studied by a light scattering technique. Macromolecules 32:7815
72. Ohkura M, Kanaya T, Kaji K (1992) Gels of poly(vinyl alcohol) from dimethyl sulphoxide/water solutions. Polymer 33:3686–3690
73. Takeshita H, Kanaya T, Nishida K, Kaji K, Takahashi T, Hashimoto M (2000) Ultra-small-angle neutron scattering studies on phase separation of poly(vinyl alcohol) gels. Phys Rev E 61:2125
74. Trieu H, Qutubuddin S (1994) Polyvinyl alcohol hydrogels I: microscopic structure by freeze-etching and critical point drying techniques. Colloid Polym Sci 272:301
75. Trieu H, Qutubuddin S (1995) Poly(vinyl alcohol) hydrogels: 2. Effects of processing parameters on structure and properties. Polymer 36:2531
76. Auriemma F, De Rosa C, Triolo R (2006) Slow crystallization kinetics of poly(vinyl alcohol) in confined environment during cryotropic gelation of aqueous solutions. Macromolecules 39:9429
77. Auriemma F, De Rosa C, Ricciardi R, Lo Celso F, Triolo R, Pipich V (2008) Time-resolving analysis of cryotropic gelation of water/poly(vinyl alcohol) solutions via small-angle neutron scattering. J Phys Chem B 112:816
78. Cahn JW (1965) Phase separation by spinodal decomposition in isotropic systems. J Chem Phys 42:93
79. Hirotsu S, Kaneki A (1988) Dynamics of phase transition in polymer gels: studies of spinodal decomposition and pattern formation. In: Komura S, Furukawa H (eds) Dynamics of ordering process in condensed matter. Plenum, Kyoto, pp 481–486
80. Takeshita H, Kanaya T, Nishida K, Kaji K (2001) Spinodal decomposition and syneresis of PVA gel. Macromolecules 34:7894
81. Wunderlich B (1980) Macromolecular physics, crystal melting, vol 3. Academic, New York
82. Grebowicz J, Cheng SZD, Wunderlich B (1986) Kinetics of transitions involving condis crystals. J Polym Sci Part B Polym Phys 24:675
83. Cheng SZD (1988) Kinetics of mesophase transitions in thermotropic copolyesters. 1: calorimetric study. Macromolecules 21:2475
84. Bao QB, Higham PA (1991) Hydrogel intervertebral disc nucleus. US5047055
85. Hyon SH, Cha WI, Oka M, Ikada Y (1993) Shock absorbing ability of joint materials. III. Effect of molecular weight and saturated water content on the loss factor of PVA-hydrogels. Polym Prep Jpn (Eng Ed) 42:71
86. Mano I, Goshima H, Nambu M (1986) New polyvinyl alcohol gel materials for MRI phantoms. Magn Reson Med 3:921
87. Kharine A, Manohar S, Seeton R, Kolkman RGM, Bolt RA, Steenbergen W, de Mul FFM (2003) Poly(vinyl alcohol) gels for use as tissue phantoms in photoacoustic mammography. Phys Med Biol 48:357
88. Takamura A, Ishii T, Hidaka H (1992) Drug release from poly(vinyl alcohol) gel prepared by freeze-thaw procedure. J Control Release 20:21
89. Peppas NA, Scott JE (1992) Controlled release from poly(vinyl alcohol) gels prepared by freezing-thawing processes. J Control Release 18:95
90. Ficek BJ, Peppas NA (1993) Novel preparation of poly (vinyl alcohol) microparticles without crosslinking agent for controlled drug delivery of proteins. J Control Release 27:259
91. Gutiérrez MC, Aranaz I, Ferrer ML, del Monto F (2010) Productions and properties of poly (vinyl alcohol) hydrogels: recent developments. In: Mattiasson B, Kumar A, Galaev IY (eds)

Macroporous polymers: production, properties and biological/biomedical applications. CRC, Boca Raton, p 83
92. Podorozhko EA, D'yakonova EA, Kolosova OY, Klabukov LF, Lozinsky VI (2012) A study of cryostructuring of polymer systems. 34. Poly(vinyl alcohol) composite cryogels filled with microparticles of polymer dispersion. Colloid J 74:708
93. Podorozhko EA, Vorontsova TV, Lozinsky VI (2012) Study of cryostructuring of polymer systems. 32. Morphology and physicochemical properties of composite poly(vinyl alcohol) cryogels filled with hydrophobic liquid microdroplets. Colloid J 74:110
94. Lozinsky VI, Zubov AL, Titova EF (1997) Poly(vinyl alcohol) cryogels employed as matrices for cell immobilization. 2. Entrapped cells resemble porous fillers in their effects on the properties of PVA-cryogel carrier. Enzyme Microb Technol 20:182
95. Podorozhko EA, Korlyukov AA, Lozinsky VI (2010) Cryostructuring of polymer systems. XXX. Poly(vinyl alcohol)-based composite cryogels filled with small disperse oil droplets: a gel system capable of mechanically induced releasing of the lipophilic constituents. J Appl Polym Sci 117:1332.
96. Abitbol T, Johnstone T, Quinn TM, Gray DG (2011) Reinforcement with cellulose nanocrystals of poly(vinyl alcohol) hydrogels prepared by cyclic freezing and thawing. Soft Mater 7:2373
97. Pan Y, Xiong D, Chen X (2007) Mechanical properties of nanohydroxyapatite reinforced poly (vinyl alcohol) gel composites as biomaterial. J Mater Sci 42:5129
98. Lozinsky VI, Damshkaln LG (2001) Study of cryostructuration of polymer systems. XX. Foamed poly(vinyl alcohol) cryogels. J Appl Polym Sci 82:1609